

UNCLASSIFIED

AD 272 681

*Reproduced
by the*

**ARMED SERVICES TECHNICAL INFORMATION AGENCY
ARLINGTON HALL STATION
ARLINGTON 12, VIRGINIA**



**THE ORIGINAL PRINTING OF THIS DOCUMENT
CONTAINED COLOR WHICH ASTIA CAN ONLY
REPRODUCE IN BLACK AND WHITE**

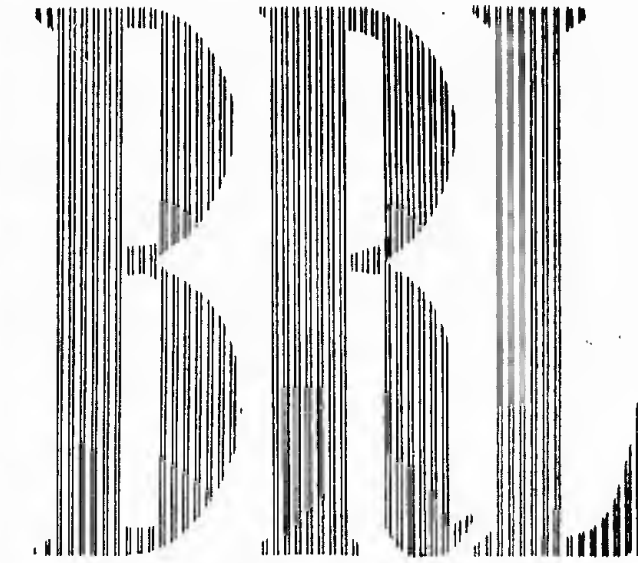
UNCLASSIFIED

NOTICE: When government or other drawings, specifications or other data are used for any purpose other than in connection with a definitely related government procurement operation, the U. S. Government thereby incurs no responsibility, nor any obligation whatsoever; and the fact that the Government may have formulated, furnished, or in any way supplied the said drawings, specifications, or other data is not to be regarded by implication or otherwise as in any manner licensing the holder or any other person or corporation, or conveying any rights or permission to manufacture, use or sell any patented invention that may in any way be related thereto.

ORIGINAL CONTAINS COLOR PLATES: ALL ASTIA
REPRODUCTIONS WILL BE IN BLACK AND WHITE.
ORIGINAL MAY BE SEEN IN ASTIA HEADQUARTERS.

CATALOGED BY ASTIA
IS AD NO.

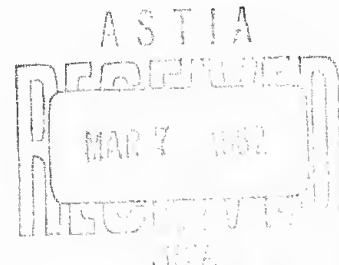
272681



MEMORANDUM REPORT NO. 1381
DECEMBER 1961

MECHANICS OF CRATER FORMATION IN
SAND AND CLAY PRODUCED BY
UNDERGROUND EXPLOSIONS

W. H. Townsend
Mark Langseth
B. Perkins, Jr.



Department of the Army Project No. 503-04-002
Ordnance Management Structure Code No. 5010.11.815
BALLISTIC RESEARCH LABORATORIES



ABERDEEN PROVING GROUND, MARYLAND

BALLISTIC RESEARCH LABORATORIES

MEMORANDUM REPORT NO. 1381

DECEMBER 1961

MECHANICS OF CRATER FORMATION IN SAND AND CLAY PRODUCED BY
UNDERGROUND EXPLOSIONS

W. H. Townsend
Mark Langseth
B. Perkins, Jr.

Terminal Ballistics Laboratory

Department of the Army Project No. 503-04-002
Ordnance Management Structure Code No. 5010.11.815

ABERDEEN PROVING GROUND, MARYLAND

B A L L I S T I C R E S E A R C H L A B O R A T O R I E S

MEMORANDUM REPORT NO. 1381

WHTownsend/MLangseth/BPerkins,Jr/iv
Aberdeen Proving Ground, Md.
December 1961

MECHANICS OF CRATER FORMATION IN SAND AND CLAY PRODUCED BY
UNDERGROUND EXPLOSIONS

ABSTRACT

Studies of crater dimensions versus shot depth have been made for sand and clay. By using a colored column technique, true crater dimensions and depths have been measured. Mineral and moisture content have been held nearly constant. Shear strength, grain size, soil density, cohesion and plasticity were measured. Accelerations of the ground particle versus distance were measured for shot depths varying from zero to 2 units of scale distance. The values of the acceleration at a given distance from successive explosions at the same depth had an average deviation from the mean value of approximately 25 per cent for both sand and clay. The average deviation of the crater dimensions was less than 10 per cent from the mean for sand and less than 5 per cent for clay.

TABLE OF CONTENTS

	Page
INTRODUCTION	9
PROCEDURE	10
Shot Area Layout for Sand	12
Shot Area Layout for Clay	12
Crater Measurement	12
Soil Tests	14
Acceleration Measurements	14
Analysis of Acceleration Records	15
Definitions of Terms Relating to Crater Formations	15
Rupture Zone	15
Fracture Zone	15
Plastic Zone	15
Elastic Zone	15
True Crater	16
Cavity and Funnel	16
RESULTS	18
Crater Measurements	18
Profile of True Craters in Sand and Clay	18
True Crater Radius vs Shot Depth	18
True Crater Depth vs Shot Depth	21
Soil Tests	21
Acceleration Measurements: Sand	24
Peak Resultant Accelerations	24
Acceleration vs Time Plots	24
Pulse Velocities	25
Acceleration Measurements: Clay	25
Peak Resultant Accelerations	25
Peak Resultant Accelerations vs Distance	25
Accelerations vs Time Records	30
Mechanism of Crater Formation	30
DISTRIBUTION LIST	77

LIST OF TABLES

	Page
1. Crater Measurements and Soil Characteristics (Sand)	41
2. Crater Measurements and Soil Characteristics (Clay)	42
3. Peak Acceleration vs Distance in Sand.	43
4. Peak Acceleration vs Distance in Clay.	44

LIST OF FIGURES

	Page
1. Sand Box Set Up.	11
2. Shot Set Ups for Sand and Clay	13
3. Nomenclature of Excavated Crater	17
4. Scale Crater Radius vs Scale Shot Depth in Sand.	19
5. Scale Crater Radius vs Scale Shot Depth in Clay.	20
6. Ratio of True Crater Radius to True Crater Depth in Sand . . .	22
7. Ratio of True Crater Radius to True Crater Depth in Clay . . .	23
8. Peak Resultant Acceleration vs Distance in Sand.	26
9. Peak Resultant Acceleration vs Distance in Clay.	27
10. Peak Resultant Acceleration vs Distance in Clay.	28
11. Acceleration vs Time in Clay	29
12. The Story of Crater Formation.	32
13. Typical Crater in Sand Illustrating Use of Colored Columns . .	33
14 - 17. Excavated Craters in Sand	47 - 50
18 - 23. Excavated Craters in Clay	51 - 56
24. Typical True Crater Profiles in Sand	57
25. Typical True Crater Profiles in Clay	58
26 - 34. Accelerations vs Time in Sand	61 - 69
35 - 41. Accelerations vs Time in Clay	70 - 76

INTRODUCTION

The radius of the crater formed by an explosive is a criterion for predicting damage to underground structures. If the mechanisms of crater formation were fully known, crater dimensions and damage for any particular type and amount of explosive could be estimated. The first comprehensive study of crater formation in soil was conducted during World War II by a Princeton University Research Group under the leadership of C. W. Lampson. (1) A large volume of data was obtained on the transient and permanent effects of underground explosions. Dr. Lampson formulated empirical equations utilizing factors affecting the stress wave close to an explosion. Empirical equations were given for the peak pressure, impulse, particle velocity, accelerations, and displacements as a function of distance, depth of burial of charge and gage, and the type of soil. Similar relations between crater size and the shot parameters were deduced.

Numerous groups have carried on this work since World War II. In 1946-47 a large program was conducted in the Canal Zone. (5) Charges of TNT weighing from 8 to 200 lbs were fired at various depths in the principal soil formations in the vicinity of the canal, and both the apparent and true craters were measured. These crater measurements in a wide variety of soils, from marine muck to basalt, supported the empirical relations of Lampson.

Recent crater studies have been coordinated with nuclear tests in the western United States. Foremost among the H. E. studies were the underground explosion tests by Engineering Research Associates under the auspices of the U. S. Army Engineers, and the Mole Program of the Stanford Research Institute under the auspices of AFSWP (now DASA). This work has not only produced a large quantity of useful data, but has also resulted in greatly improved and refined measuring techniques. These tests were carried out with a wide variety of charge sizes and at many test locations, consequently, the data varies over a wide range.

The crater study at BRL was undertaken to advance the basic understanding of the mechanics of crater formation. Small scale tests permitted better control of the factors influencing the size and shape of craters and improved techniques increased the reproducibility of the data.

PROCEDURE

In 1954, BRL initiated the present crater program in which 1/4-lb charges of 50/50 pentolite were detonated at depths from 0 to 2 lambda* in two basic types of soils: sand and silty clay. The small scale of these tests allowed a large number of shots to be handled in a small area. As a result, soil conditions were more uniform and could be checked after each test firing. Furthermore, the program developed a new technique for measuring craters more accurately.⁽³⁾ This technique used vertical colored columns of sand which were inserted into the soil at three inch intervals from the charge center (Appendix A). When the half of the crater on one side of the line of colored columns is carefully excavated after the shot, the permanent ground displacements and true crater dimensions can be accurately and easily measured. These parameters can then be related to the various crater determining factors. The following soil characteristics were determined at each location: moisture content, soil density, shear strength, cohesion, grain size, and plasticity. The particle acceleration close to the explosion was measured at five distances from the charge center (2 to 6 lambda). Three accelerometers were mounted at each distance. They were mutually perpendicular so that the horizontal, transverse and vertical acceleration could be measured simultaneously. From the acceleration vs time records made for each test shot, the attenuation of the peak acceleration with distance was determined. Other observable characteristics such as pulse velocity and pulse shape change with distance were recorded but no detailed analysis was made of this data for this report.

Measurements were taken in sand and in clay. The colored columns were inserted at three-inch intervals from the shot center, by forcing a sharpened 1/2-inch rod through a jig (Figure 1) into the medium. The holes were then filled alternately with black, red, and blue sand, beginning with the black sand in the center hole.

* Lambda is a unit of scaled distance, the length of which, in feet, is numerically equal to the cube root of the weight of explosive in pounds.

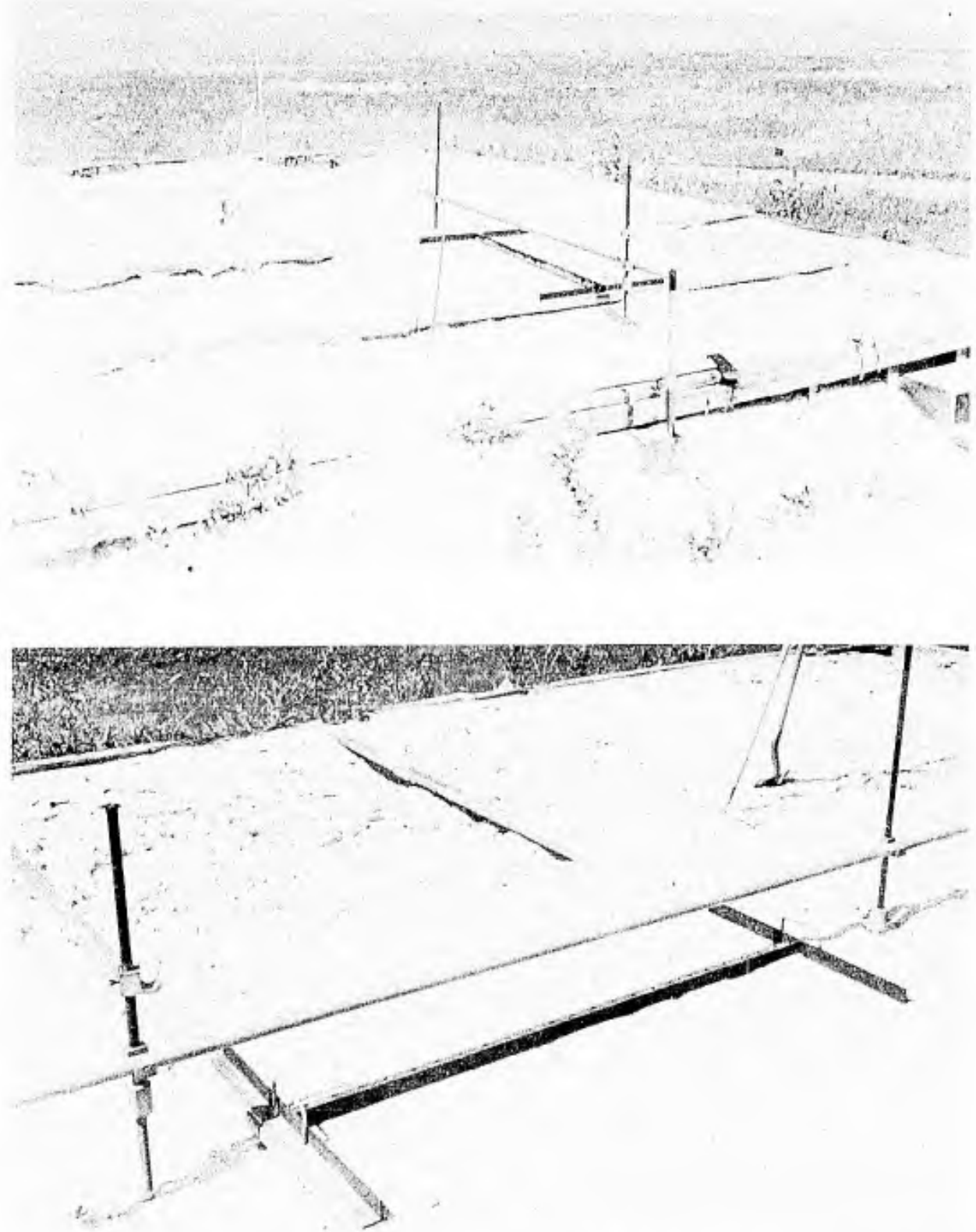


FIGURE 1. SAND BOX SHOWING JIG FOR COLORED COLUMNS

The accelerometers were placed a foot below the surface at five distances from the shot center varying from 2 to 6 lambda in a fan-shaped array (see Figure 2). Finally, the pentolite sphere and detonator were placed at the selected depth, the medium was replaced in the charge holes and tamped to restore the original density. A total of 82 usable records were obtained.

Shot Area Layout for Sand

All of the sand crater shots were fired in a large sandbox 25 x 26 x 6 feet located on Spesutie Island. This box was filled with sifted sand. The soil characteristics of the sand are given in Appendix A, Table I.

Since the detonation of a quarter-pound charge affects an area approximately five feet in radius, four separate test areas could be set up in the box at one time. After the four test shots were fired, the sand had to be completely reworked to a depth of approximately four feet. By removing the top four feet and then replacing it in six inch layers, each carefully rolled, the original condition was closely duplicated. The last layer was leveled with a bar sliding along two level steel rails mounted on the rim of the box and the box was then divided into four quadrants and the center of each square was chosen for the charge hole.

Shot Area Layout for Clay

An area at the test site on Spesutie Island was chosen for the clay shots. The first foot of topsoil was removed. The next four feet of silty clay at this site are remarkably uniform. The soil characteristics of this clay are given in Appendix A, Table II. The test area was large enough to accommodate all the test shots.

Crater Measurement

After the shot had been fired, an excavation was made along one side of the colored columns such that all the columns of colored sand were exposed. Such an excavated crater is shown in Figure 3. A reference rod was then placed over the colored columns, and leveled. A plumb bob was dropped from this rod so that it coincided with the original central column.

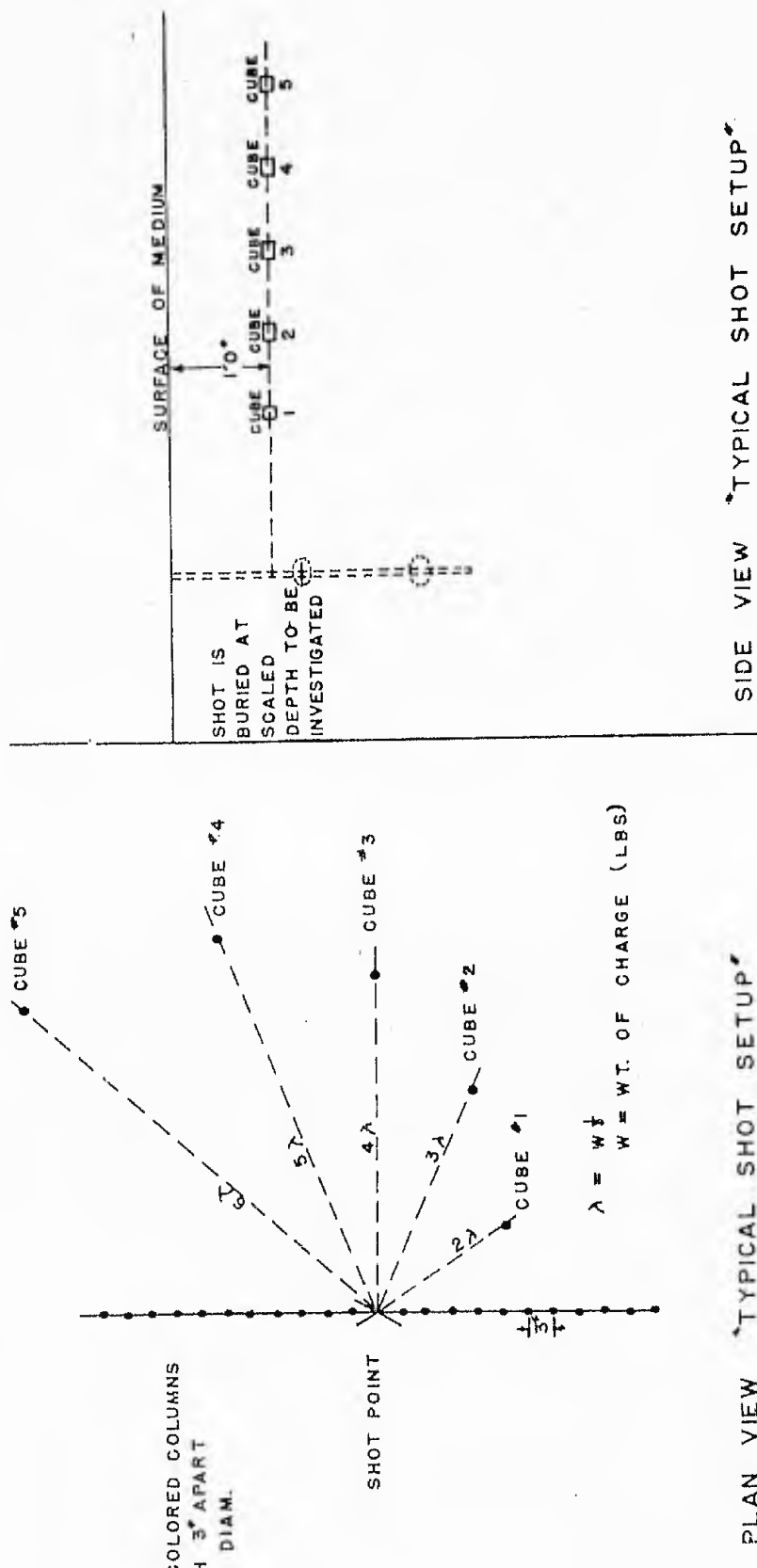


FIGURE 2. TYPICAL SHOT SETUPS FOR SAND AND CLAY

The horizontal coordinates of the true crater profile were determined by measuring the distances from the plumb line to the point of shear on the colored columns. The vertical coordinates were determined by measuring the vertical distances from the horizontal rod to the shear in each column. Photographs of the excavated craters are shown in Appendix B.

Soil Tests

The sample of soil was taken from the shot area by gently driving a bevelled brass tube horizontally into the soil at about shot depth but far enough away from the charge center so that the ground was undisturbed. This sample was sealed and sent to the U. S. Bureau of Public Roads who conducted tests for density, shear strength, moisture content and grain size.

Acceleration Measurements

The accelerometers used in this program were small piezo-electric gages manufactured by Gulton Laboratories. Because of their small size and rugged construction, these gages were ideal for small-scale, close-in measurements.

The accelerations were recorded with an Armour Research Oscillographic Unit.* The unit is housed in a mobile trailer so that it could be moved close to the shot area. Low-noise cable was used to transmit the signal from the accelerometer to the amplifiers in the trailer. After amplification, the signal was presented on 15 three-inch oscilloscopes and recorded by 4 high-speed strip film 35mm cameras.

At each of the five distances, 2, 3, 4, 5 and 6 lambda, three of the accelerometers were mounted perpendicular to one another in a 2-inch aluminum cube. This arrangement allowed the three components of acceleration (horizontal, vertical and transverse) to be measured simultaneously at each distance. The average density of the cube, containing the accelerometers, was adjusted to match the density of the sand and the clay, so as to provide the best coupling of the ground and the accelerometers. Each cube was buried 12 inches below the surface. The five cubes were arranged in a fan-shaped array to provide an undisturbed path between the shot center and the cubes.

* Final Report Project No. 90-624E Mobile Oscillographic Measuring Unit.
Armour Research Foundation of Illinois Institute of Technology.

Analysis of Acceleration Records

The 35mm acceleration records acquired from the shots fired in the program were read on an IBM Telecordex reader. Trace displacements were measured every 1/10 millisecond and punched on cards. These cards were then processed in the ORDVAC computer to calculate the actual acceleration for a given trace displacement. These accelerations in turn were punched on separate cards, which could be transcribed to acceleration versus time plots by an automatic plotter.

Definitions of Terms Relating to Crater Formation

In order to facilitate discussion a few definitions are necessary. Many terms have been used to describe craters. The terms defined in the following paragraphs are used in this report.

When a charge is detonated in soil or rock a spherical compression wave travels out from the charge. The surrounding material suffers a degree of deformation which depends on its distance from the exploding charge as the shock wave passes through. The zones in which the various degrees of deformation occur are:

1. Rupture Zone - The region immediately adjacent to the charge out to a radius of about $1-1/2$ lambda in which the soil or rock is completely fragmented and broken free from the surrounding consolidated material.
2. Fracture Zone - The portion of the medium between $1-1/2$ to 3 lambda which usually remains intact after an explosion except for numerous shear and radial fractures.
3. Plastic Zone - The region about 3 to 10 lambda where the soil is permanently displaced outwardly from the charge center, but no fractures are discernible.
4. Elastic Zone - The region beyond about 10 lambda where the soil or rock has not been permanently deformed by the passage of the compression wave.

5. The True Crater - An excavated crater clearly shows the boundary between the rupture and the fracture zone. Inside this boundary the soil or rock has been completely sheared from the surrounding material. The profile of this boundary is called the "True Crater".

True Crater Diameter is the average diametric measured at the intersection of the true crater and the original ground level. The vertical distance from the original ground level to the deepest point in the true crater is the true crater depth.

The true crater profile is easily seen in photographs of the excavated craters in this report by connecting the points at which the colored columns are sheared, as is shown in Figure 3.

6. Cavity and Funnel - Two additional terms are useful in describing true craters; the cavity and funnel. See Figure 3.

The cavity defines the bottom portion of the true crater and is a remnant of the nearly spherical hollow space forged in the soil by the expanding high pressure gases before they vented to the open air.

The funnel refers to the remainder of the true crater. It is formed by the shearing away of material by the expanding explosive products as they vent to the air.

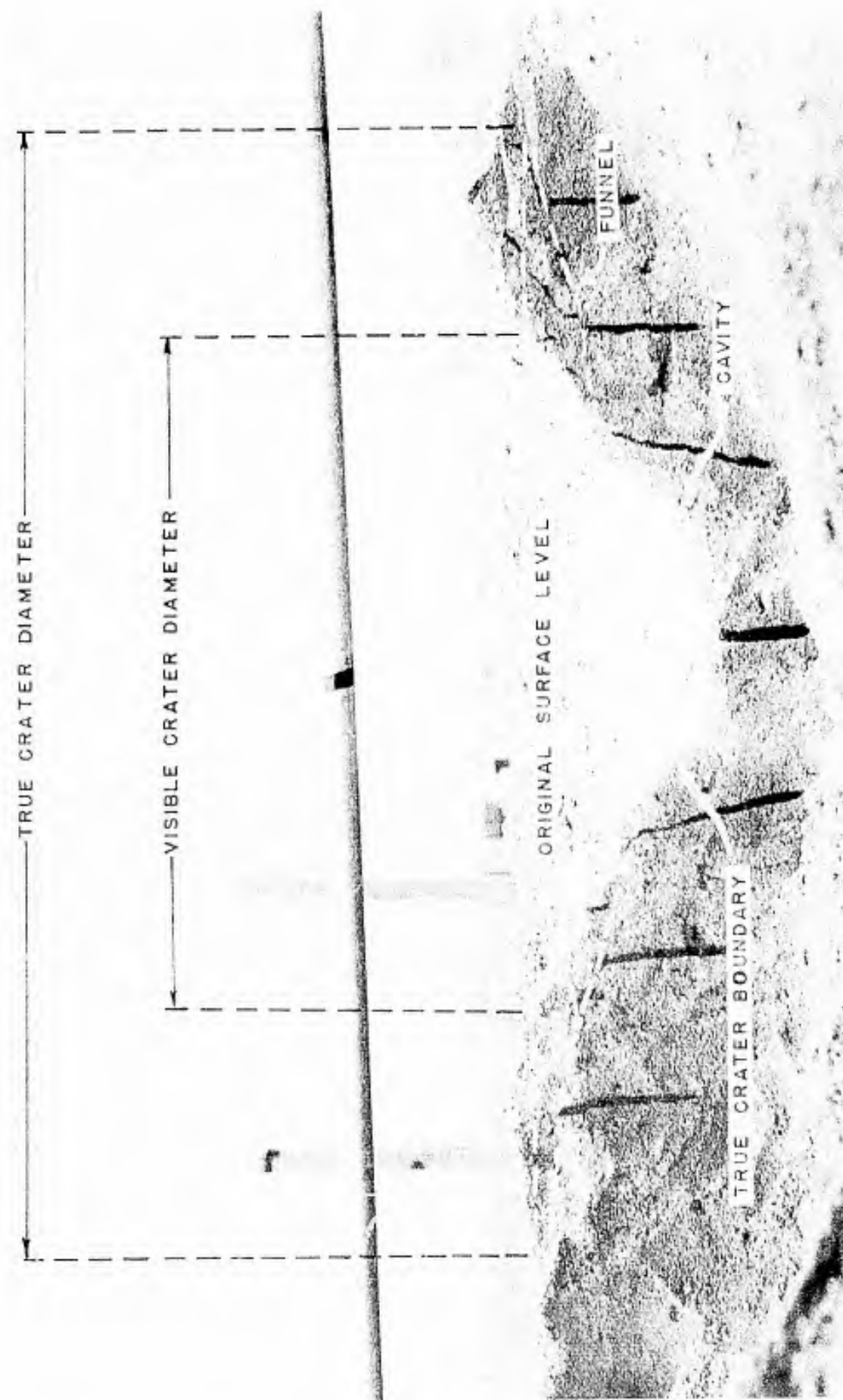


FIGURE 3. NOMENCLATURE OF EXCAVATED CRATER

RESULTS

The crater profiles, soil test tabulations and acceleration versus time plots have been compiled in Appendices A, B, and C. Representative data and plots showing the relation of crater dimensions to charge depth and the variation of acceleration of the ground particle with distance from the explosion are given below.

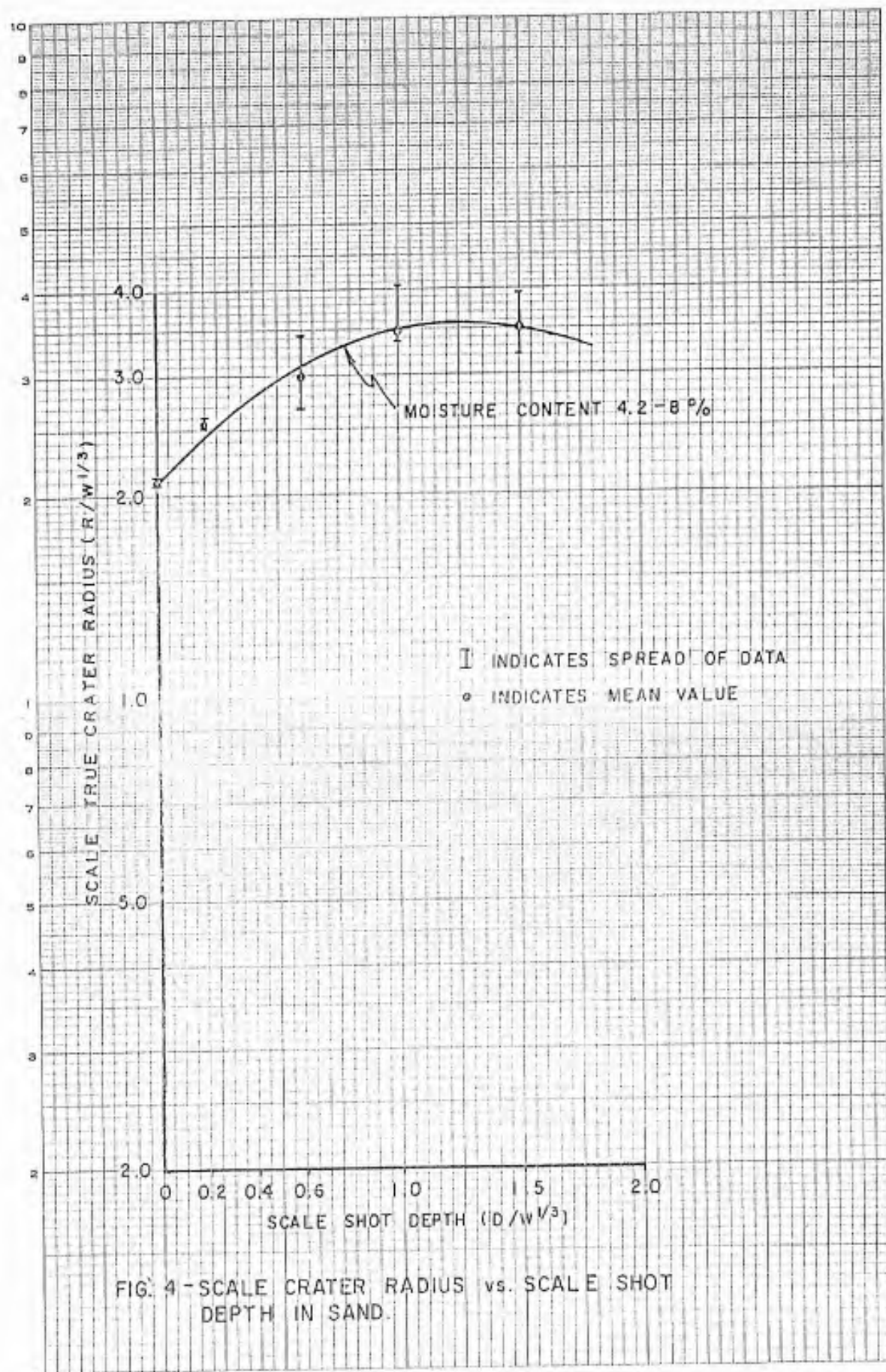
Crater Measurements

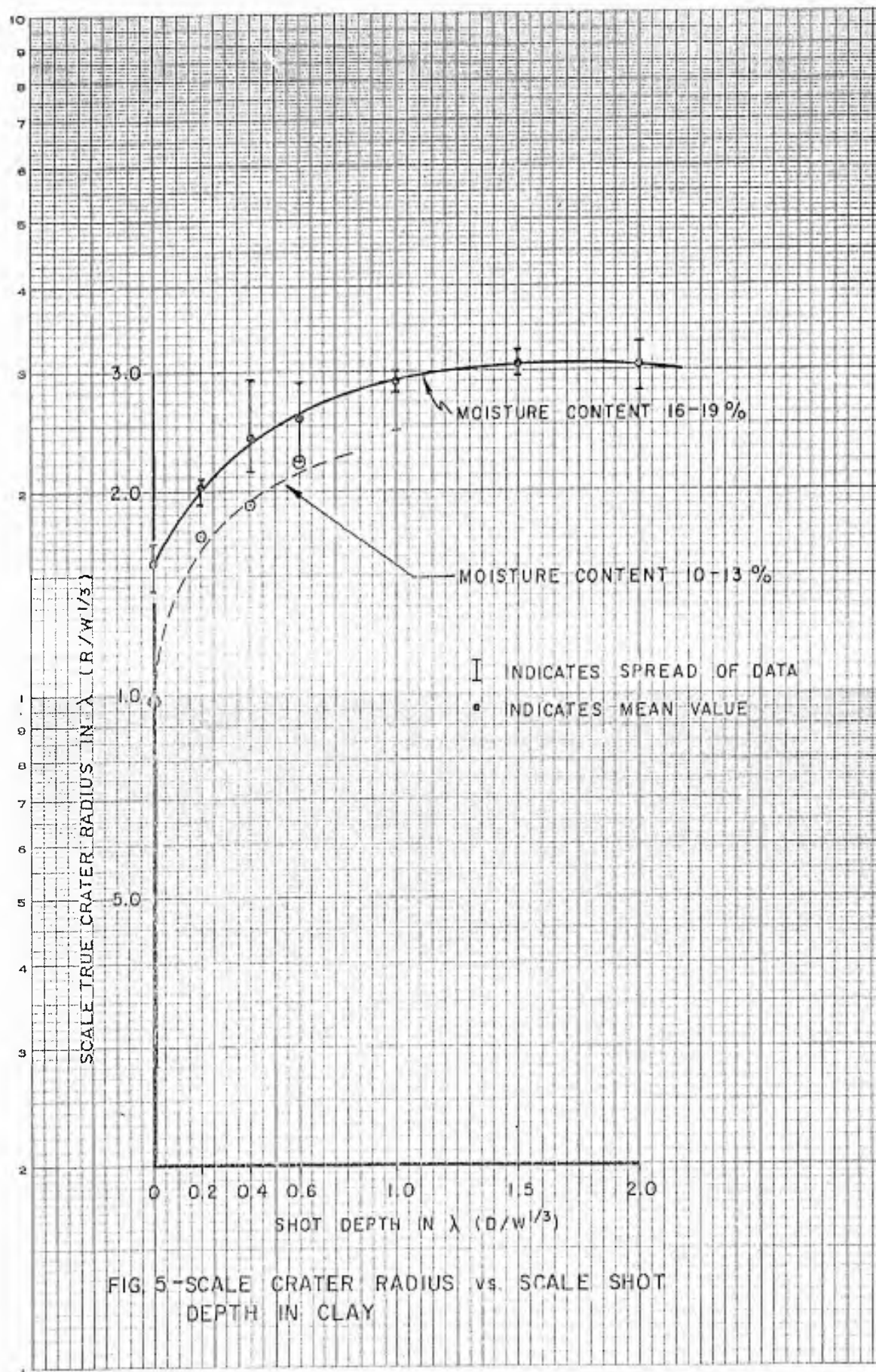
Profile of True Craters in Sand and Clay. In the two types of soil tested, the true crater profiles exhibited distinctly different shapes. In sand, the profile was generally smooth. Below the charge center the crater is roughly hemispherical, while above the charge the sides of the crater flare to less steep angles (see Appendix B, Figure 14 through 17). Near the surface the angle that the sides make with the horizontal decreases rapidly toward zero.

The clay craters, on the other hand, showed a very distinct break between the cavity and funnel. In Appendix B, Figures 18 through 23 present pictures of the excavated craters. In several craters the loose material has been scooped away to expose the charred walls and spherical shape of the cavity. Above the cavity a strong, almost horizontal, shear zone extends out into the consolidated material. Above this main shear is the large bowl-shaped funnel which constitutes the main volume of the true crater. The sides of the funnel are usually poorly defined and for the deeper shots the slope of the sides becomes steeper near the surface and nearly vertical at ground level.

True Crater Radius versus Shot Depth. With a given charge size and soil type, the radius of the true crater will vary as shown by the curves in Figures 4 and 5. The shape of the curve and the magnitude of the radii shown will vary slightly with the type of soil tested.

In sand the moisture content varied from 4.2% to 8.0% and the crater radius varied from 2.1 lambda for shots at the surface to 3.8 lambda for shots at a scale depth of 1.6 lambda. At shot depths greater than 1.5 lambda the true crater radius slowly decreased until a camouflet was formed.





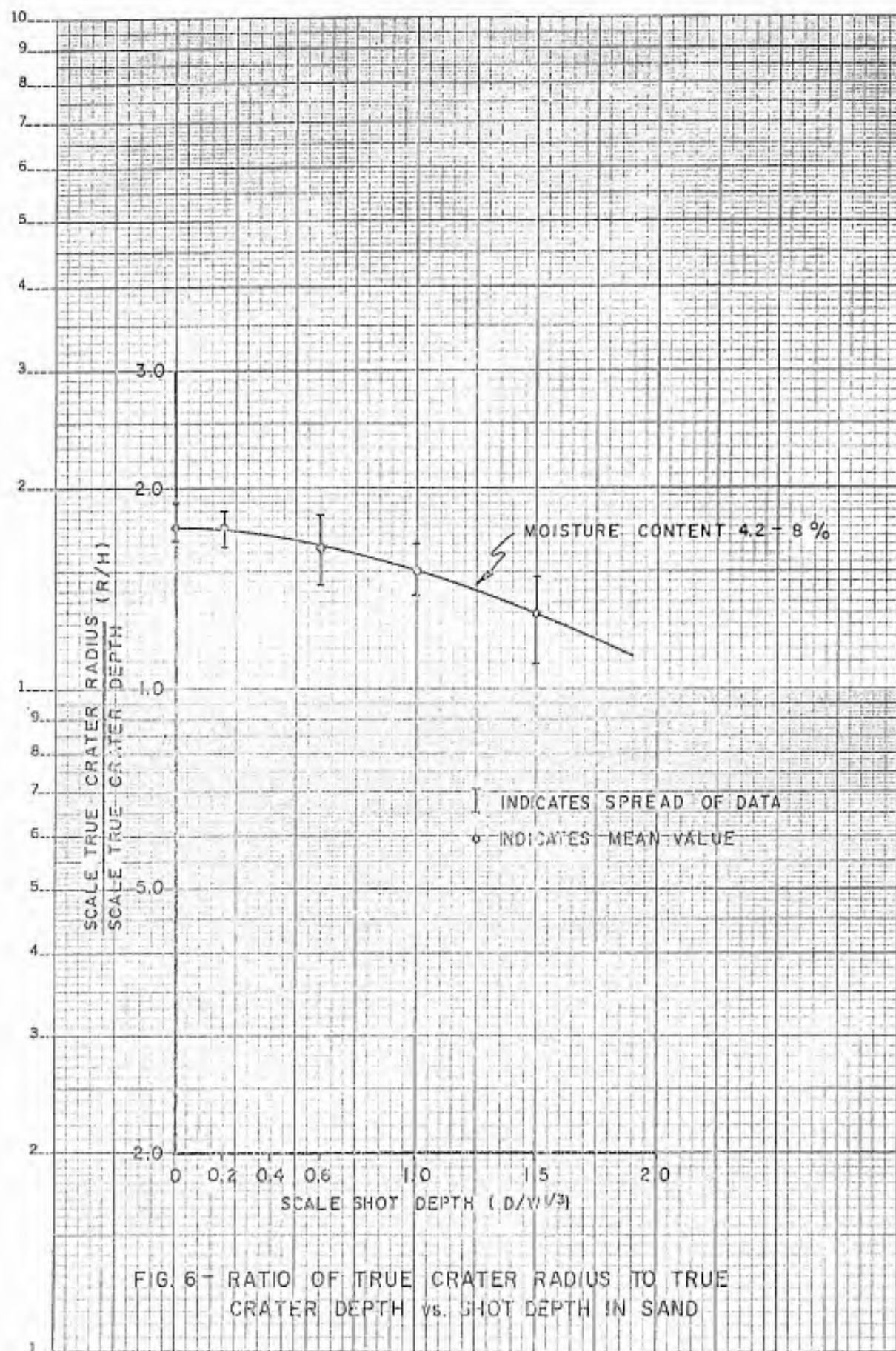
The true crater radius in clay is generally smaller than in sand because of the greater shear strength in clay. The range of values for clay obtained in these tests was from 0.98 lambda with a moisture content of 10-13% at 0.0 shot depth, to 3.1 lambda with moisture content of 16 to 19% at a scale shot depth of 1.5 lambda. The crater radius decreased to about 3 lambda for charges buried at a depth of 2 lambda. The plot of the scale true crater radius versus scale shot depth is presented in Figure 5. The solid curve shows the scale crater radius for a moisture content of 16-19% while the dashed curve presents data for a moisture content of 10-13%.

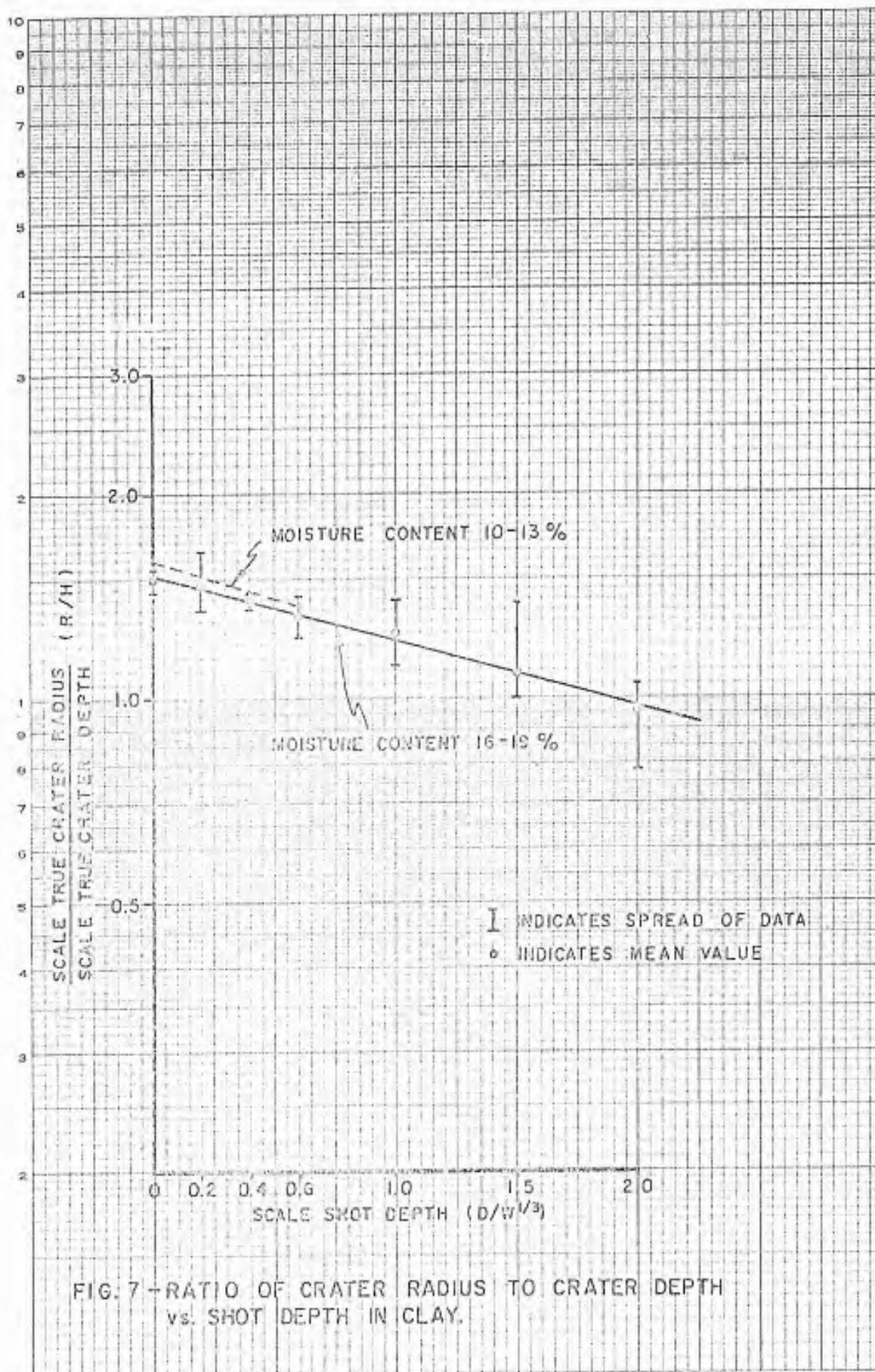
True Crater Depth Versus Shot Depth. The values of scale crater depth for various scale shot depths for explosions in sand and in moist clay are shown in Tables 1 and 2 and the ratios of radius to depth for True Craters in sand and in clay are shown in Figures 6 and 7.

The scale crater depth in sand is greater than in clay for corresponding shot depths and the ratios of radius to depth is greater for sand than for the clay. The factors determining these dimensions are discussed in the section on mechanism of crater formation.

Soil Tests. A tabulation of the results of the soil tests carried out by the Bureau of Public Roads on the sand samples is given in Appendix A, Table 1. Eight samples of the sand were tested and all gave remarkably uniform results. The moisture content was nearly constant (approximately 6%) throughout most of the test program. There was a small increase in moisture content toward the end of the program, but no appreciable variation of crater dimensions could be correlated with the observed increase. Other quantities measured, such as angle of friction, cohesion, coefficient of friction remained relatively constant. The grain size was found to be nearly uniform with 98% passing a 2mm sieve, 68% passing a 0.42mm sieve and 9% passing 0.074mm sieve.

Tabulation of the soil test results on the clay are given in Appendix A, Table 2. The characteristics of the clay are reasonably uniform. However the moisture content suffered a severe decrease between Shot No. 19 and Shot





No. 20. A period of several weeks of very dry weather elapsed between these shots and the moisture content of the clay dropped from about 18% to about 11% and the shear strength, as indicated by the values of cohesion, approximately doubled.

The effect of this change on the magnitude of the crater radius is clearly depicted by the dashed curve in Figure 5.

Acceleration Measurements: Sand,

Peak Resultant Acceleration (sand). At any one distance from the charge the resultant peak acceleration varied about 25% from the mean value of acceleration at that distance. In view of the variables in these tests from shot to shot such as tamping of the shot and the instruments, moisture content, this amount of variation is to be expected.

The peak accelerations for distances from the shot of 2 to 6 lambda are presented in Appendix A, Table III. The plots of peak resultant acceleration versus distance from the charge center for each shot depth tested are shown in Figure 8. In most cases a straight line could be fitted to the points on a log-log plot. The slopes of these lines indicate that the peak resultant acceleration in sand varies as the -4.3 power of the distance from the charge.

Acceleration Versus Time Plots (sand). The acceleration versus time records are reproduced in Figures 26 through 34 in Appendix C. In each figure the horizontal, transverse and vertical components are shown together. The time and acceleration scales are identical for the three components, but differ for various gage distances.

The acceleration pulses occurring at a distance of 2 lambda for the deeper shot depths have an average rise time of approximately 2000 G/millisecond and duration of the positive phase of about 1 millisecond. As the distance from the charge increases the pulse length becomes greater and the shape becomes more symmetrical. At 6 lambda from the charge center the length of the positive phase is 4-1/2 to 5 milliseconds with a rise time of 4 G/millisecond.

For sand most of the records show only a positive phase of the acceleration pulse. The deceleration phase of the ground motion has been lost or inaccurately recorded probably because of a base line drift. However, the acceleration records taken in clay with the same equipment had strong negative phases. Since the plastic deformation of sand is so much greater than that of clay it is suspected that the deceleration phase of the motion of the sand particle may be of such low magnitude that it is imperceptible in the records.

Pulse Velocities (sand). The velocity of propagation of the acceleration pulses was determined by plotting the time of first energy arrival against distance. The gages used were too insensitive to detect energy moving from grain to grain so that the determined velocities would represent the velocities of propagation of the plastic wave in the sand. The average velocity in sand of the acceleration pulse was approximately 550 ft/second.

Acceleration Measurements: Clay.

Peak Resultant Accelerations (clay). The acceleration records taken during the clay test program were more satisfactory than those in sand. A tabulation of peak resultant accelerations in clay is given in Appendix A, Table IV. These values are approximately twice those observed in sand. The average deviation from the mean value at a given distance and shot depth was about 22%.

Peak Resultant Acceleration Versus Distance (clay). The log-log plots of peak resultant accelerations in clay versus distance from the charge are seen in Figure 9 and 10. The observed values are best fitted by a broken line which would indicate a change in physical properties with depth and resulting refraction of the seismic pulse.

As in the case of sand (Figure 5), the slope of the acceleration versus distance curve determines the exponent of r in the expression:

$$A_r = A_0 r^{-n} \quad (1)$$

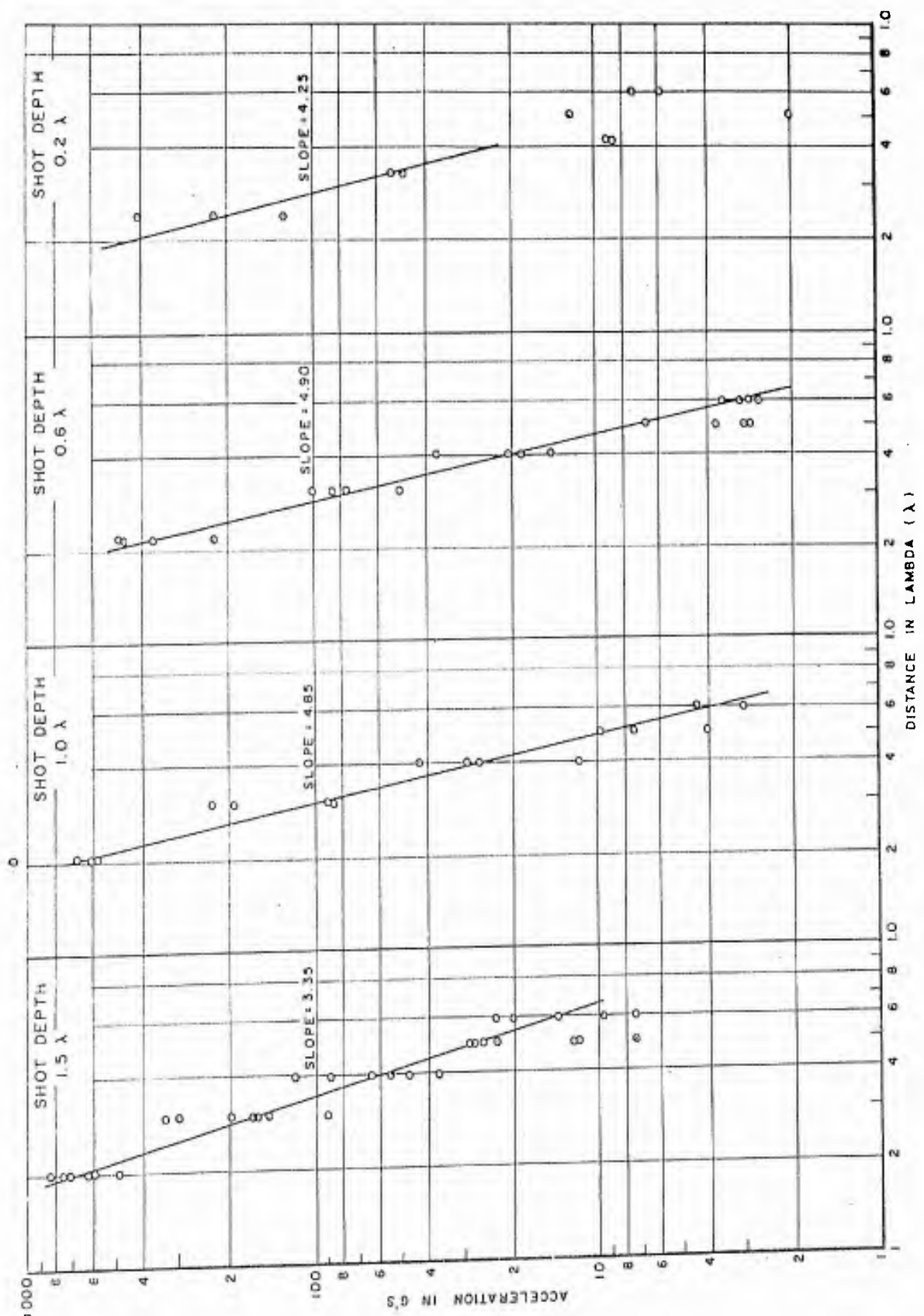


FIGURE 8 - PEAK RESULTANT ACCELERATION vs. DISTANCE IN SAND

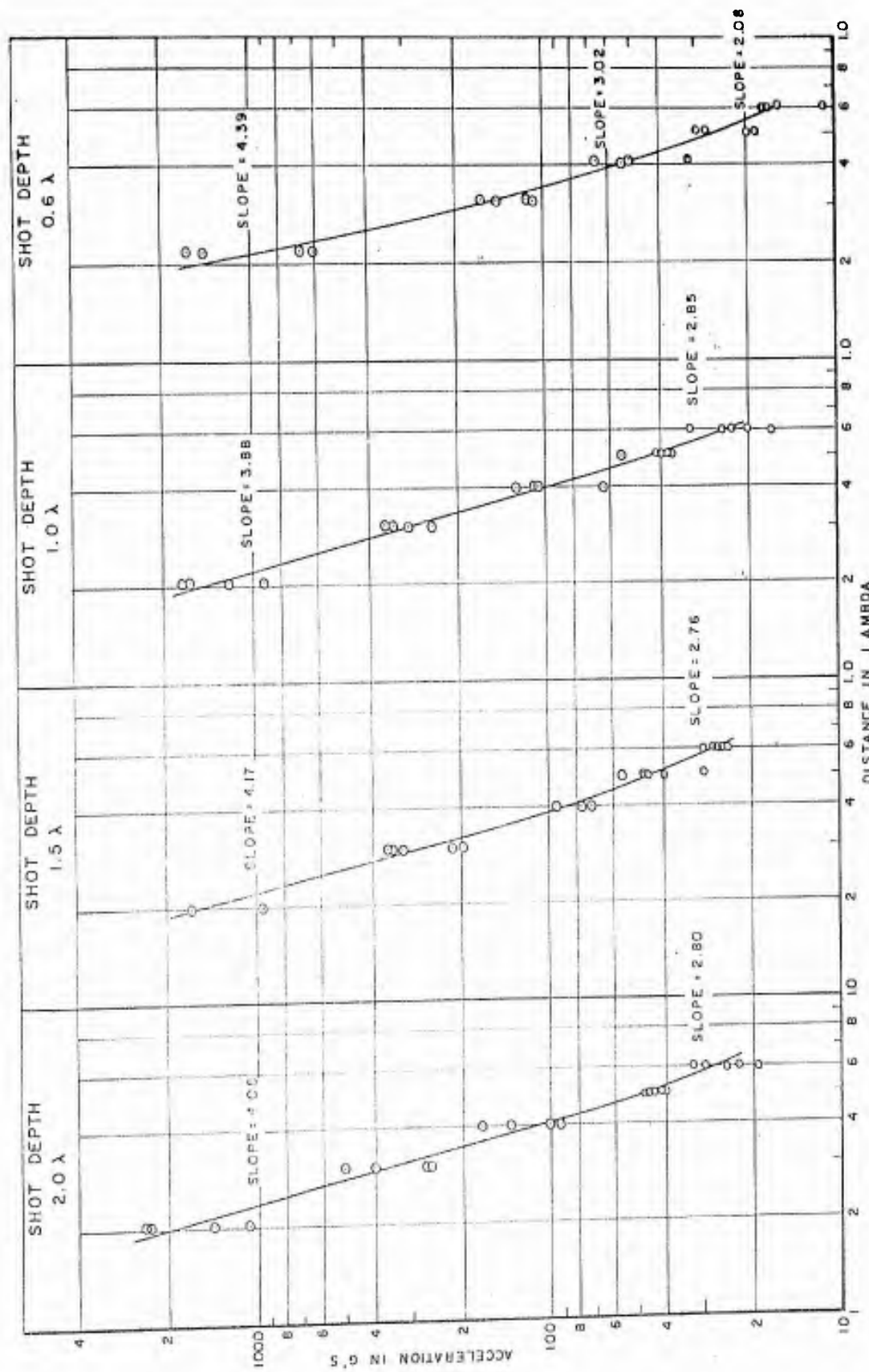


FIGURE 9-PEAK RESULTANT ACCELERATION vs. DISTANCE IN CLAY

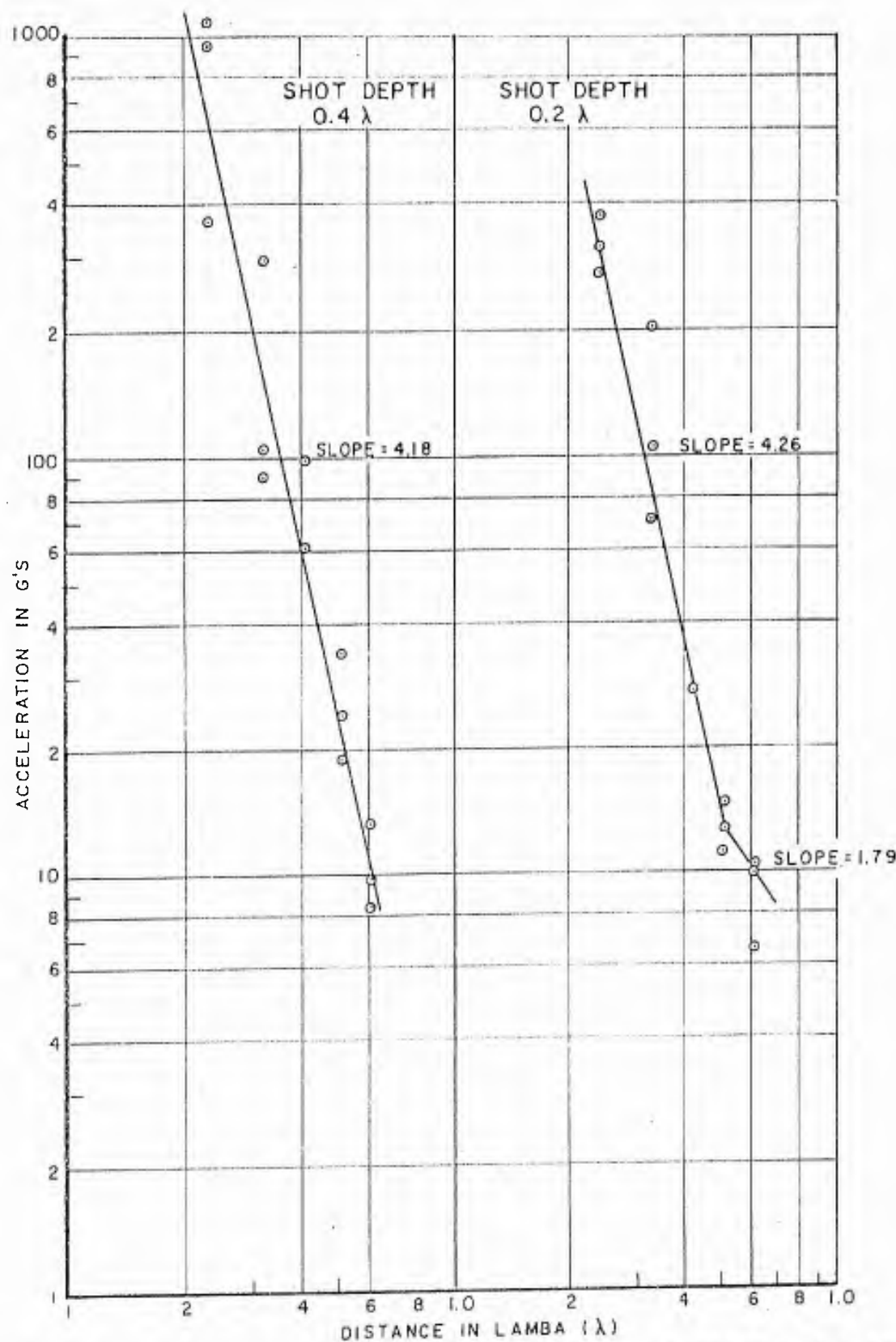


FIGURE 10-PEAK RESULTANT ACCELERATION vs. DISTANCE IN CLAY

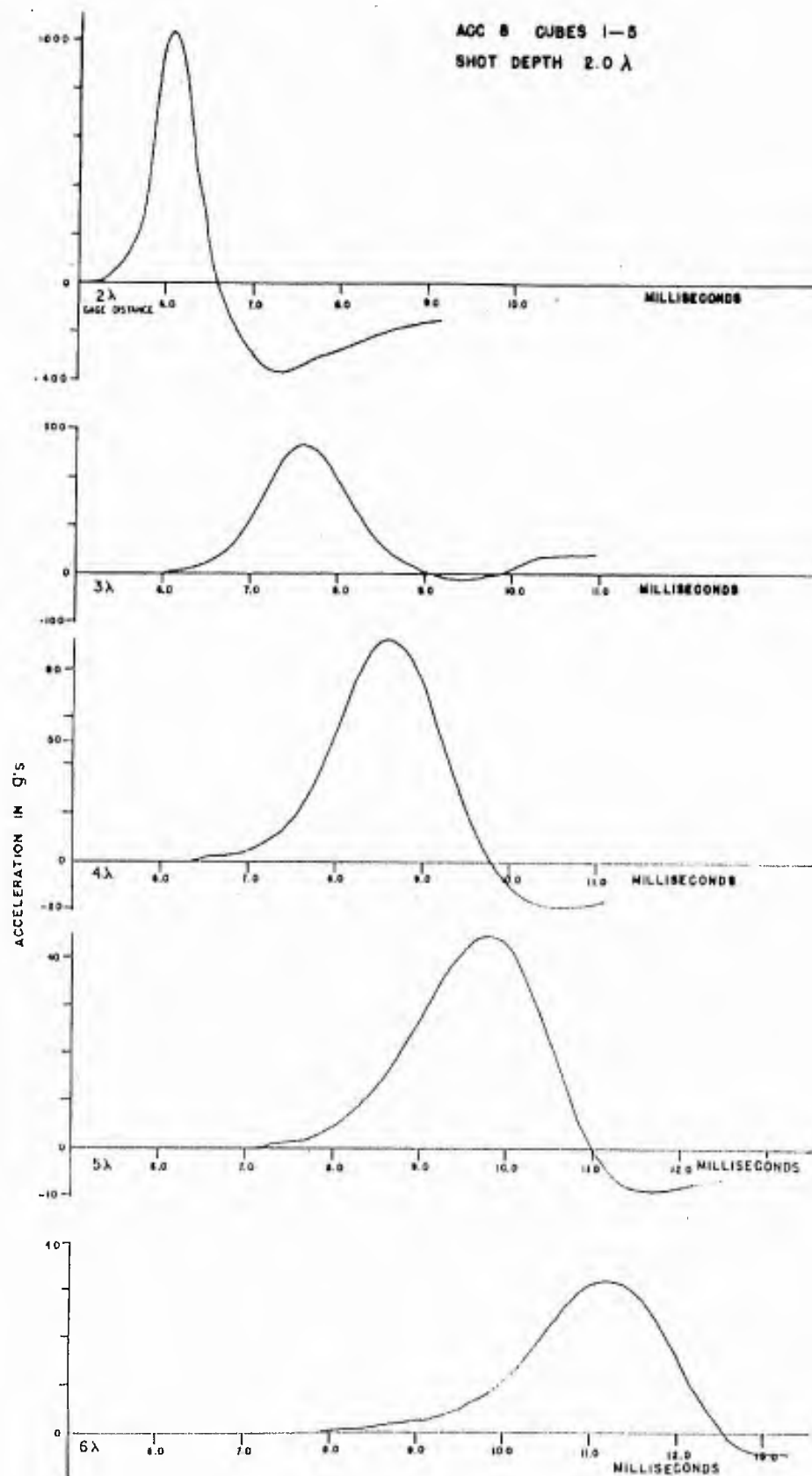


FIGURE 11 - ACCELERATION vs. TIME IN CLAY

where

A_0 = initial acceleration

A_r = acceleration at distance r

n = exponent determining rate of decrease of acceleration
with distance.

The average values of n in clay are 4.16 for the short distances where the propagation paths are shallow and 2.86 for the greater distances where the paths are deeper. These compare with the value of 4.3 found for sand.

Acceleration vs Time Records. The acceleration versus time records from the clay tests are presented in Figures 35 through 41 in Appendix C. As in the sand plots there was a very strong base line shift after the signal was received. A rough base line correction may be made by redrawing the base lines at such an angle that the area under the positive and negative portions of the curve are equal. Figure 12 is a composite picture made from records of horizontal acceleration versus time at distances of 2 to 6 lambda. As occurred in the sand the pulse length in clay increases from about 1 millisecond at a distance of 2 lambda to about 4-1/4 milliseconds at 6 lambda. A very conspicuous precursor can be seen developing with increasing distance. The velocity of this precursor is about 1050 feet per second which agrees with the velocity of low amplitude seismic energy as determined in the laboratory for the same material.

Mechanism of Crater Formation. A study of the profiles of the craters resulting from shots varying in depth from 0 to approximately 2 lambda reveals the probable mechanism of crater formation. The soil immediately below the shot is compressed, forming a hemispherical cavity, while the soil to the side is scoured out by the expanding gas. When the explosion occurs at a depth of 0.5 lambda or less the true crater is formed almost entirely by the scouring action, i.e., there is practically no "cavity" formed and the crater is saucer shaped. For explosions at a depth of 0.6 lambda or greater a hemispherical bowl shape, the "cavity", is formed with its center at the shot location and extending downward while from the shot location to the surface the soil is scoured out by the expanding gas. A study of Figures 24 and 25 in Appendix B will substantiate the above statements.

In the case of the shallow shots the energy apparently is released to the atmosphere before the expanding gas has time to do the work of compression on the soil. The shots at a depth of 0.4 lambda in clay show a slight "cavity" probably due to greater shear strength confining the explosion for a longer time than for a similar shot in sand. For shot depths increasing from 0 to 0.6 lambda the depth of the crater increases due to the increase in depth of both the funnel and the "cavity". From shot depths greater than 0.6 lambda the radius of the "cavity" remains essentially constant and the increase in depth of the crater is due to the increase in depth of the funnel. Therefore the slope of the curve relating depth of crater to shot depth changes in slope at a shot depth of about 0.6 lambda.

In Figure 12 the evolution of a crater is depicted.

The mechanism of crater formation has been deduced from a study of high speed cinema photographs, and the movement of the soil as depicted by the colored columns. It is believed that the following sequence of events result from the explosion of a charge positioned between the surface and about 3 lambda deep. A narrow cone of material above the exploding charge is thrown high into the air while the expanding gas pushes down on the soil below the charge compacting it and forming a hemispherical cavity. At the same time the gas is pushing out to all sides fracturing the medium close by and rupturing more distant medium to a distance of about 2 lambda from the charge. The fractured material is pushed up at an angle to the horizontal until some of it rests on the original ground surface. This material forms the lip of the crater. With the release of the gases to the atmosphere some of the fractured material slides back to the bottom of the cavity. Some of the material in the air above the crater is pushed laterally by the expanding gas. These particles fall to the surface forming a superficial layer over and beyond the lip.

The surface over which the fractured material was pushed to form the lip, is the boundary of the True Crater.

The dimensions of this crater will depend on the shear strength and compaction of the medium and a coefficient of absorption of the energy of the pressure pulse. Other factors may become apparent with further study.

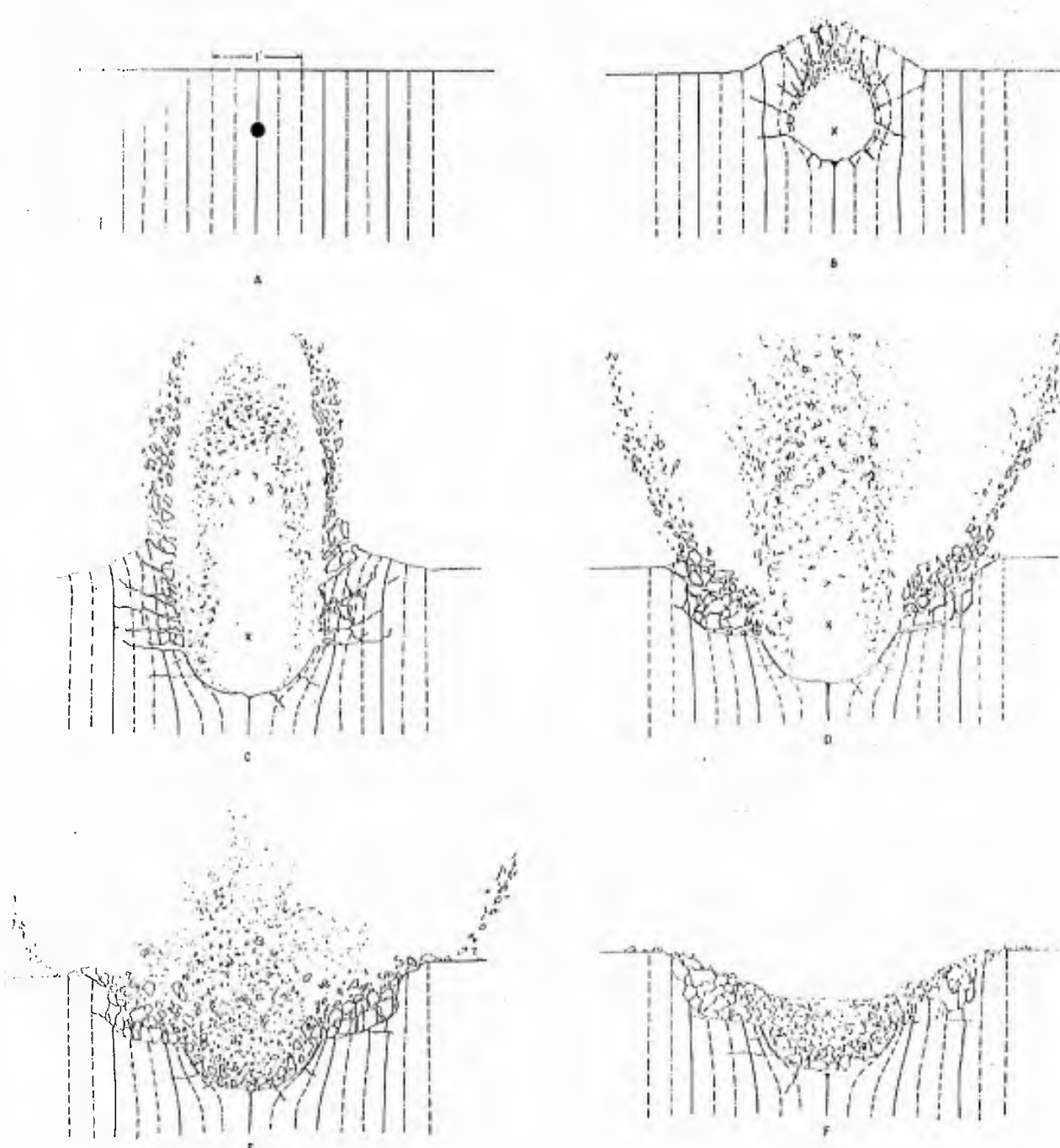


FIGURE 12—THE STORY OF CRATER FORMATION
DERIVED FROM FASTAX CAMERA
PICTURES AND THE COLORED COLUMN
TECHNIQUE.

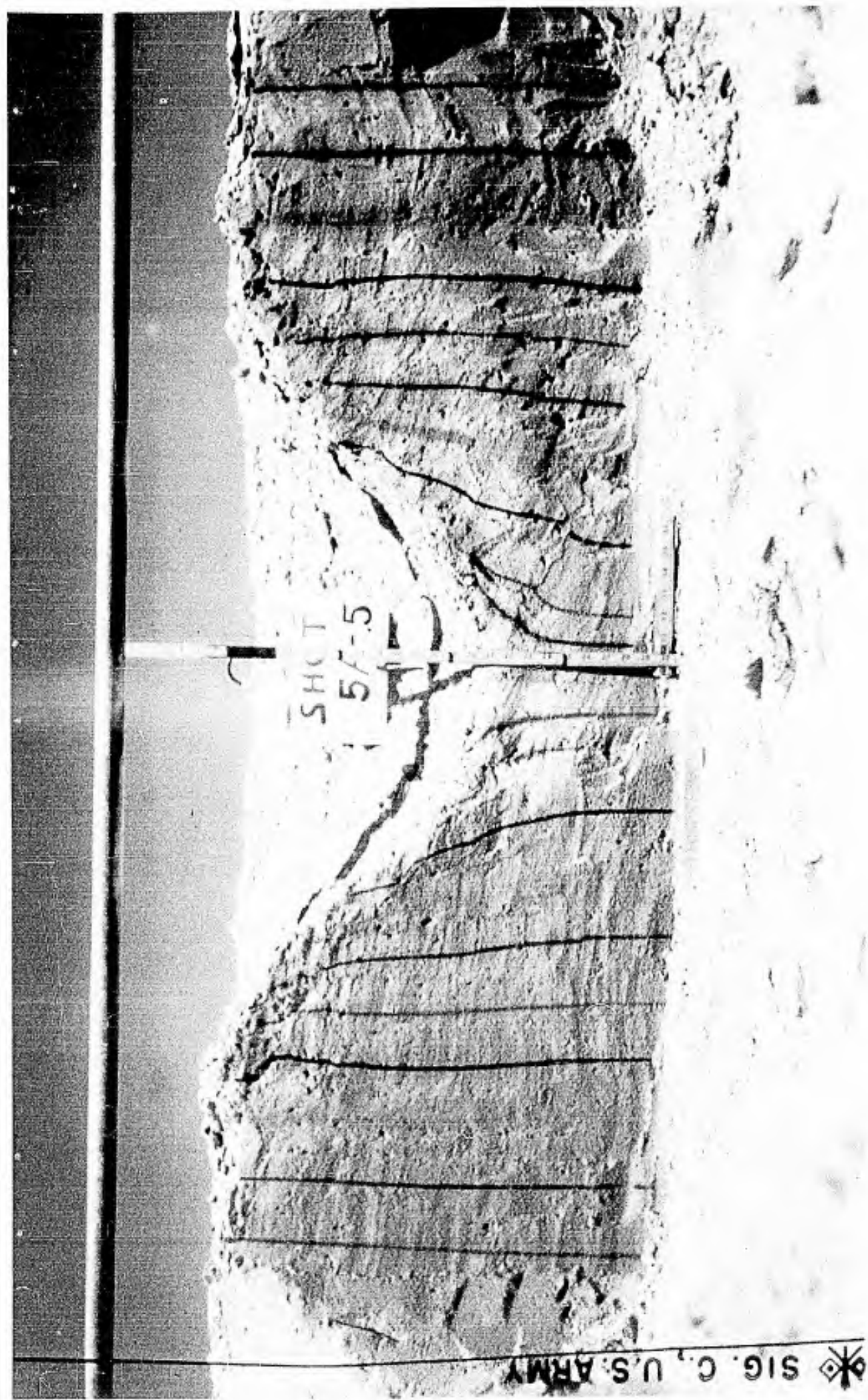


FIGURE 13 - TYPICAL CRATER IN SAND ILLUSTRATING USE OF COLORED COLUMNS.

ACKNOWLEDGMENTS

The work reported herein extended over a period of four and one-half years and involved several changes of personnel who were inducted into the military service for short periods. The care exercised by these men which is evidenced by the consistency of the data is gratefully acknowledged. The participants in the program were - W. Murphy, H. Essig, M. Ackerman, and D. Hensen.

Special appreciation must be expressed for the care and ingenuity exercised by Willis F. Jackson and W. Kurlans in providing calibration methods and maintaining the electronic instrumentation used in the acceleration measurements.

W. H. Townsend
W. H. TOWNSEND

MARK LANGSETH

B. Perkins, Jr.
B. PERKINS, Jr.

REFERENCES

1. Lampson, C. W. Final Report on Effects of Underground Explosions. National Defense Research Committee NDRC Report No. A-479, March 1946.
2. Stanford Research Institute. Small Explosion Tests, Phase II-B of Project Mole. AFSWP-290, December 1954, (Confidential).
3. Perkins, B. A New Technique for Studying Crater Phenomena. Aberdeen Proving Ground, BRL Technical Note No. 880, March 1954.
4. U. S. Special Engineering Division. Crater Tests in Residual Clay. Panama Canal Zone, ICS Memo 287-P, May 1948.
5. U. S. Special Engineering Division. Crater and Slope Tests With Explosives. Panama Canal Zone, ICS Memo 282-P, June 1948.

APPENDICES

- A. Tables
- B. Crater Profiles
- C. Accelerations vs. Times

APPENDIX A

TABLES

1. Crater Measurements and Soil Characteristics in Sand.
2. Crater Measurements and Soil Characteristics in Clay.
3. Peak Resultant Accelerations in G's vs Distance in Sand.
4. Peak Resultant Accelerations in G's vs Distance in Clay.

TABLE I
Crater Measurements and Soil Characteristics in Sand

ACS Shot No.	Charge Weight (lbs.)	Scale Charge Depth	Radius (ft)	Depth (ft)	Scale Radius	Crater Radius	Crater Depth	Moisture Content % Dry Soil	Coef. of Friction	Angle of Friction	Cohesion Kip/sq.ft.
1	0.25	1.5	2.09	1.84	3.31	1.09	1.47	6.65	0.50	26°35'	0.37
2	0.25	1.5	2.00	1.76	3.18	1.16	1.36	4.83	0.49	26°6'	0.42
3	0.25	1.5	2.04	1.75	3.24	1.37	1.36	3.5	0.75	36°51'	0.09
4	0.25	1.5	2.40	1.75	3.80	2.78	1.38	6.33	0.75	34°14'	0.15
5	0.25	1.5	2.46	1.78	3.91	2.83	1.28	5.5	4.4		
6	0.25	1.5	2.13	1.67	3.58	2.65	1.28	4.4			
7	0.25	1.5	2.11	1.56	3.34	2.48	1.35	4.2			
8	0.25	1.5	2.15	1.46	3.41	2.32	1.42				
9	0.25	1.5	2.25	1.65	3.57	2.62	1.36				
10	0.25	1.5	2.13	1.63	3.38	2.59	1.31				
11	0.25	1.5	2.34	1.43	3.71	2.27	1.64				
12	0.25	1.5	2.5	1.5	—	—	—				
13	0.25	1.5	2.00	1.99	3.97	3.17	—				
14	0.25	1.5	2.5	1.5	1.83	3.16	1.26				
15	0.25	1.5	2.42	1.53	3.84	2.90	1.32				
16	0.25	1.5	2.53	1.96	3.70	3.11	1.19				
17	0.25	1.0	2.16	1.50	3.46	2.36	1.43				
18	0.25	1.0	2.58	1.58	4.13	2.50	1.65				
19	0.25	1.0	2.08	1.50	3.32	2.36	1.59				
20	0.25	1.0	2.27	1.50	2.8	2.38	1.52				
21	0.25	0.6	2.02	1.27	3.18	2.02	1.59				
22	0.25	0.6	2.15	1.25	3.41	1.98	1.72				
23	0.25	0.6	2.00	1.09	3.18	1.73	1.83				
24	0.25	0.6	1.67	1.17	2.65	1.86	1.43				
25	0.25	0.6	1.67	1.35	2.65	2.14	1.24				
26	0.25	0.2	1.59	0.95	2.52	1.51	1.67				
27	0.25	0.2	1.63	0.96	2.58	1.52	1.69				
28	0.25	0.2	1.59	0.94	2.52	1.49	1.69				
29	0.25	0.2	1.61	0.87	2.55	1.38	1.85				
30	0.25	0.0	1.31	0.79	2.08	1.25	1.25				
31	0.25	0.0	1.38	0.76	2.12	1.24	1.21				

TABLE II
CRATER MEASUREMENTS AND SOIL CHARACTERISTICS IN CLAY

ACS Shot No.	Charge Wt. (lb)	Scale Charge Depth (λ)	True Radius (ft)	True Depth (ft)	Scale Crater Radius	Scale Crater Depth	Crater Radius Crater Depth (R/H)	Moisture Content % Dry Soil	Angle of Friction	Cohesion KIP Sq Ft
2	.25	2.0	2.02	2.04	3.199	3.244	.986			
3	"	2.0	1.74	2.24	2.762	3.558	.776	19	33.5	.75
4	"	2.0	1.82	2.00	2.887	3.178	.908	19	35.5	.47
6	"	2.0	2.04	1.91	3.245	3.028	1.072	18	39.8	.61
7	"	2.0	1.88	1.87	2.980	2.946	1.011	17	33.0	1.34
8	"	2.0	1.79	1.97	2.848	3.126	1.049	18	30.9	1.12
9	"	1.5	1.97	1.88	3.132	2.992	1.046	17	36.2	1.00
10	"	1.5	2.07	1.50	3.291	2.384	1.380	18	39.5	1.00
11	"	1.5	1.89	1.65	3.007	2.616	1.127	19.0	27.9	1.06
12	"	1.5	1.84	1.58	2.927	2.500	1.171	17.0	39.8	1.17
13	"	1.5	1.85	1.84	2.940	2.93	1.003	18.0	38.8	1.00
14	"	1.0	1.50	1.53	2.440	2.133	1.125	17.6	16.5	1.13
15	"	1.0	1.71	1.33	2.733	2.133	1.281	19	25.2	.78
16	"	1.0	1.79	1.39	2.867	2.233	1.284	18.6	31.5	.44
17	"	1.0	1.75	1.29	2.800	2.067	1.355	18	29.5	.66
18	"	1.0	1.67	1.53	2.667	2.133	1.250	18	28.4	.82
19	"	1.0	1.78	1.29	2.827	2.052	1.38	18	30.9	.74
*20	"	0.6	1.68	1.06	2.662	1.688	1.57	13.1	-	-
*24	"	0.6	1.34	.96	2.132	1.524	1.399	13	45.5	1.49
*25	"	0.6	1.47	.94	2.020	1.490	1.356	13	-	-
*26	"	0.6	1.42	1.00	2.251	1.590	1.416	13	39.5	2.01
*27	"	0.4	1.17	.92	1.860	1.456	1.277	13.2	-	-
*28	"	0.4	1.26	.83	2.000	1.324	1.510	12	45.1	1.24
*29	"	0.4	1.21	.92	1.920	1.456	1.318	12.6	-	-
*	"	0.4								
*31	"	0.2	1.16	.81	1.834	1.290	1.422	12.2	-	-
*32	"	0.2	1.06	.77	1.639	1.226	1.377	13.6	44.3	1.39
*33	"	0.2	1.05	1.63	1.662	.994	1.672	11.8	-	-
*34	"	0	.62	.42	.980	.662	1.480	10.9	-	-
*35	"	0	.61	.34	.967	.616	1.567	10.6	44.1	1.51
*36	"	0	.63	.35	1.000	.548	1.825	11.6	44.8	1.59
37	"	0.6	1.77	1.23	2.883	1.960	1.445	17.0		
38	"	0.6	1.65	1.22	2.633	1.947	1.340	17.0		
39	"	0.6	1.38	1.12	2.200	1.787	1.231	17.0		
40	"	0.4	1.27	.94	2.033	1.506	1.350	16.3		
41	"	0.4	1.50	1.04	2.400	1.677	1.440	16.3		
42	"	0.4	1.52	1.09	2.427	1.747	1.389	16.3		
43	"	0.4	1.83	1.29	2.933	2.067	1.419	16.3		
44	"	0.2	1.24	.87	1.987	1.387	1.433	16.5		
45	"	0.2	1.23	.87	2.053	1.387	1.480	16.5		
46	"	0.2	1.25	.87	2.000	1.387	1.442	16.5		
47	"	0.2	1.29	.78	2.067	1.253	1.649	16.5		
48	"	0	.98	.63	1.533	1.000	1.533	17.3		
49	"	0	.83	.59	1.427	.947	1.507	17.3		
50	"	0	.92	.64	1.467	1.027	1.428	17.3		
51	"	0	1.00	.67	1.600	1.067	1.499	17.3		

* These shots were repeated due to drastic change in moisture content.
The effect on the crater curve is shown in Figure 7.

TABLE III
PEAK RESULTANT ACCELERATIONS IN G'S VS DISTANCES IN SAND

ACS Shot No.	Scale Charge Depth (λ)	Charge Weight = .25 lbs.				
		Distance From Charge Center				
		2	3	4	5	6
4	1.5	609.1	199.3	47.9	-	9.8
5	1.5	-	-	54.8	23.3	-
6	1.5	-	-	118.6	-	20.4
7	1.5	493	161.7	64.0	-	35.7
9	1.5	757.2	306.7	88.8	29.0	23.7
10	1.5	-	-	-	28.1	63.3
11	1.5	-	162.1	-	26.9	14.1
13	1.5	761.9	338	37.7	12.4	7.5
14	1.5	823.2	-	-	7.431	-
15	1.5	607.6	148.9	-	12.1	-
16	1.5	716.3	91.0	-	2.59	-
17	1.0		192.4	29.09	-	2.368
18	1.0	573.8	89.8	26.9	7.51	-
19	1.0	672.2	230.6	43.05	9.947	4.418
20	1.0	588.1	87.00	11.82	4.123	-
21	0.6	366.8	76.90	14.79	2.855	3.077
22	0.6	469.4	86.18	18.79	3.711	2.610
23	0.6	225.9	191.0	37.00	-	3.584
24	0.6	164.0	100.5	20.99	6.792	3.073
25	0.6	477.5	50.23	12.12	2.818	2.874
27	0.2	403.3	48.01	8.76	12.23	-
28	0.2	223.8	25.81	9.148	-	6.42
29	0.2	127.9	53.87	-	2.044	3.939
30	0.0	64.8	-	40.88	8.330	-
31	0.0	115.8	30.71	26.67	7.656	4.615
32	0.0	91.38	42.08	15.80	2.964	5.963

TABLE IV
Peak Resultant Accelerations in G's vs Distances in Clay

ACC Shot No.	Scale Charge Depth (λ)	Charge Weight = .25 lbs.				
		Distance From Charge Center				
2	3	4	5	6		
2	2.0	-	504.2	173.6	46.8	29.8
3	2.0	2353	194.5	41.4	23.8	15.9
4	2.0	2304	400.5	101.4	40.1	22.2
5	2.0	-	-	-	-	-
6	2.0	-	501.3	136.9	48.0	24.8
7	2.0	1410.9	261.4	-	41.2	19.4
8	2.0	1071.0	270.1	93.1	44.6	32.4
9	1.5	-	199.1	-	39.9	26.6
10	1.5	-	354.3	76.7	56.0	29.3
11	1.5	-	341.4	94.2	47.8	26.8
12	1.5	1671	319.9	-	46.3	24.3
13	1.5	950.1	213.0	70.8	29.1	25.0
14	1.0	-	-	-	-	-
15	1.0	1203	242.6	-	36.9	16.7
16	1.0	-	333.6	127.5	54.5	31.7
17	1.0	1625	357.2	107.4	41.0	20.0
18	1.0	921.9	155.0	63.5	37.7	23.0
19	1.0	1750	298.9	108.1	39.8	24.4
20	0.6	670.7	107.3	66.1	27.3	17.3
21	0.6	1627	147.3	50.7	29.6	15.1
22	0.6	1422.7	113.7	51.7	18.4	17.1
23	0.6	602.3	164.3	31.5	19.8	10.7
24	0.4	957.9	106.5	61.0	25.1	9.8
25	0.4	413.0	90.3	-	19.1	8.4
26	0.4	1064	296.1	90.9	34.0	13.3
27	-	-	-	-	-	-
28	0.2	512.0	71.1	27.1	12.8	10.5
29	0.2	375.7	107.1	-	14.6	10.2
30	0.2	272.2	205.1	-	11.4	6.6
31	0	235.4	94.0	52.8	11.8	5.4
32	0	256.1	103.6	-	19.6	12.3
33	0	239.2	-	-	15.7	10.2

APPENDIX B

CRATER PROFILES

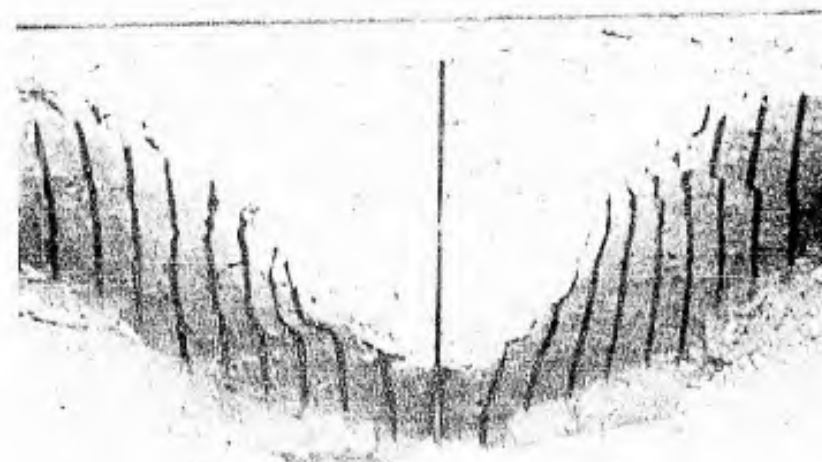
1. Excavated Craters in Sand.
2. Excavated Craters in Clay.
3. Typical True Crater Profiles in Sand.
4. Typical True Crater Profiles in Clay.



CHARGE DEPTH = 1.5λ

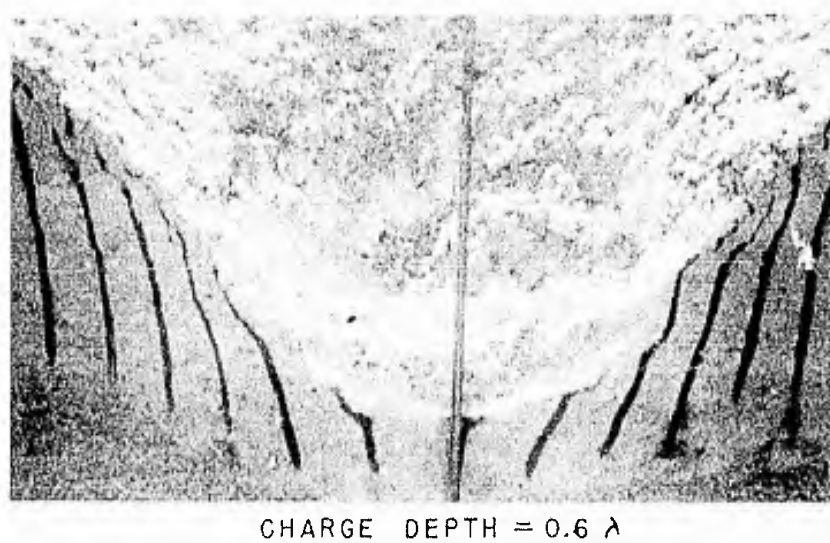


CHARGE DEPTH = 1.5λ

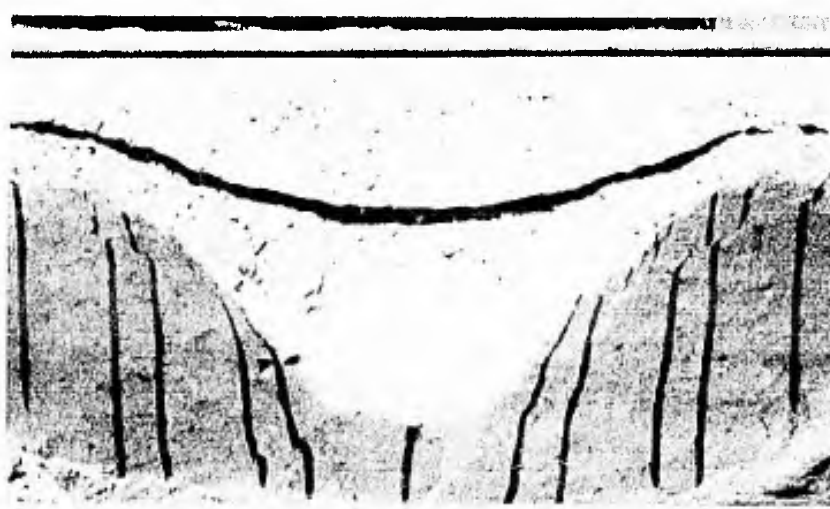


CHARGE DEPTH = 1.0λ

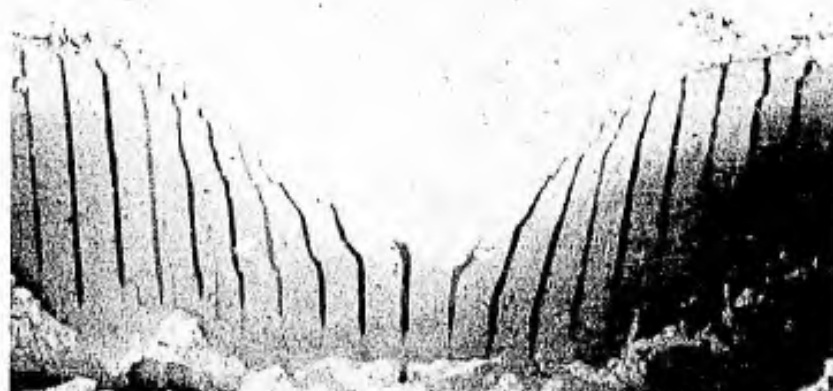
FIGURE 14-EXCAVATED CRATERS IN SAND



CHARGE DEPTH = 0.6λ



CHARGE DEPTH = 0.6λ



CHARGE DEPTH = 0.6λ

FIGURE 15 - EXCAVATED CRATERS IN SAND



CHARGE DEPTH = 0.6 λ

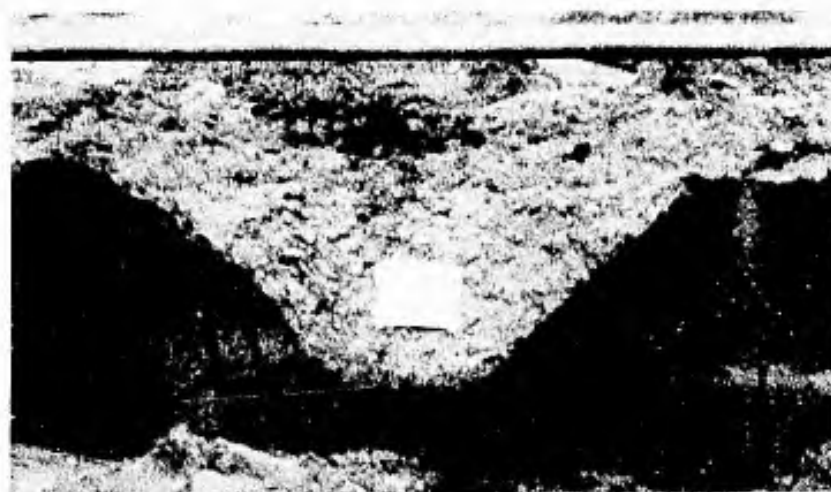


CHARGE DEPTH = 0.6 λ



CHARGE DEPTH = 0.2 λ

FIGURE 16-EXCAVATED CRATERS IN SAND



CHARGE DEPTH = 0.2 λ



CHARGE DEPTH = 0.0 λ

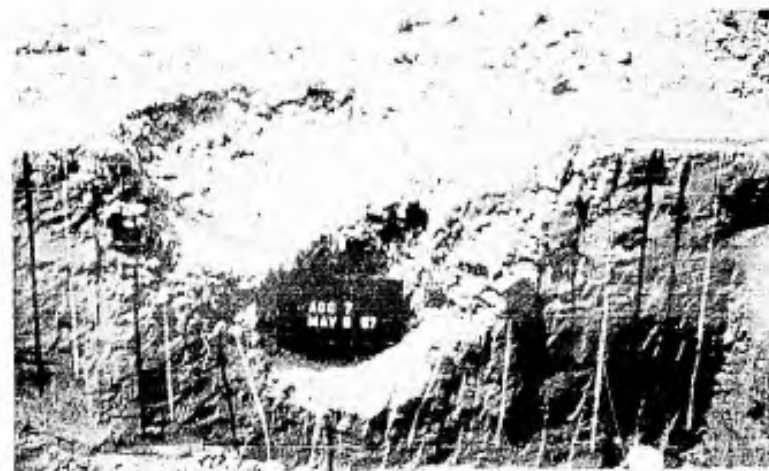


CHARGE DEPTH = 0.0 λ

FIGURE 17-EXCAVATED CRATERS IN SAND



CHARGE DEPTH = 2λ

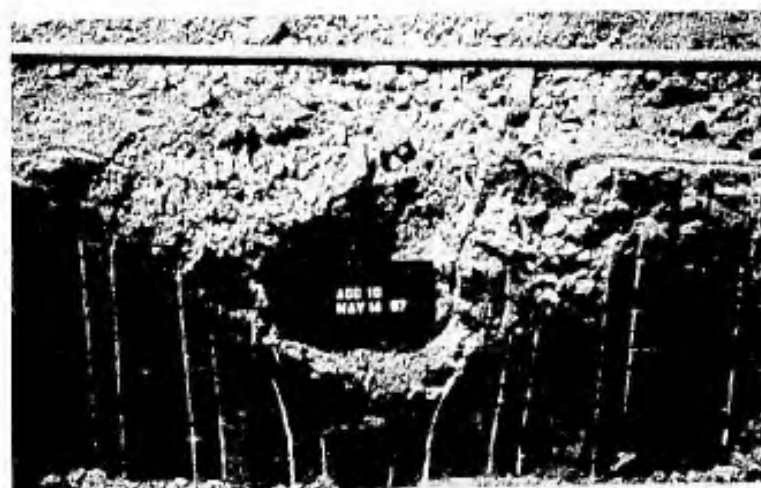


CHARGE DEPTH = 2λ

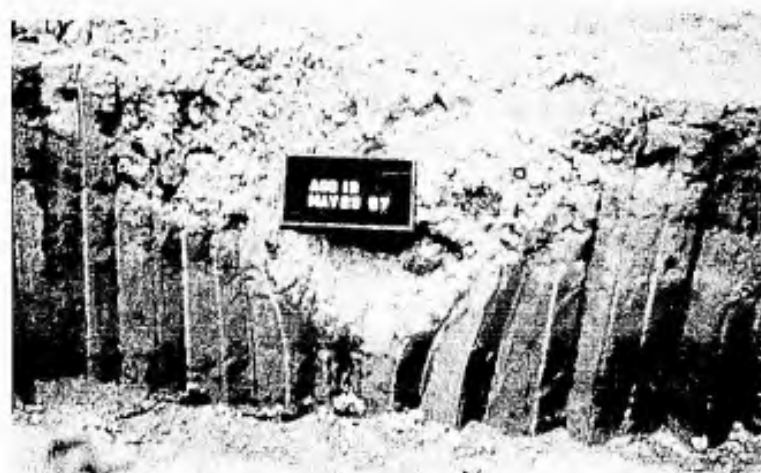


CHARGE DEPTH = 2λ

FIGURE 18-EXCAVATED CRATERS IN CLAY



CHARGE DEPTH = 1.5 λ

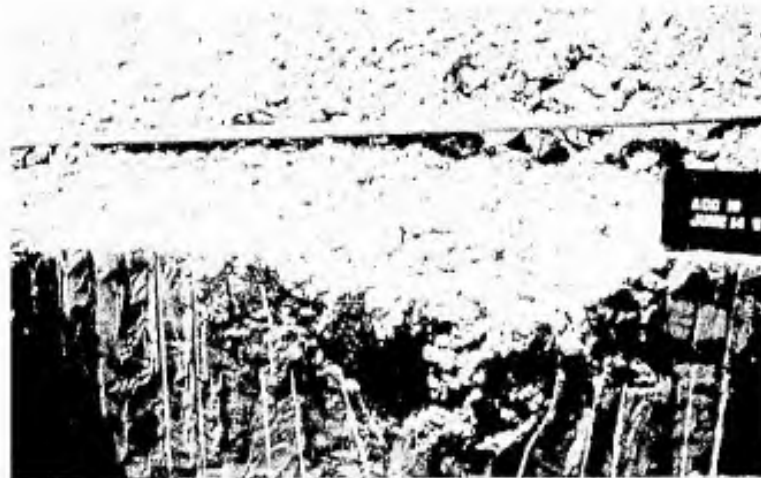


CHARGE DEPTH = 1.5 λ

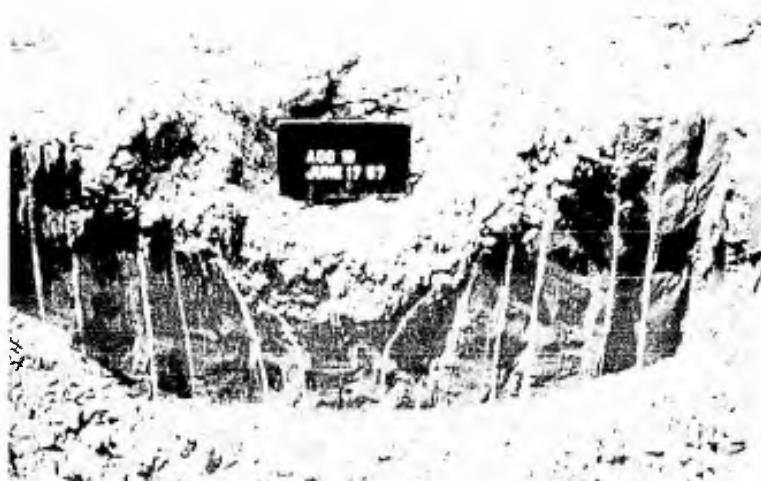


CHARGE DEPTH = 1.0 λ

FIGURE 19-EXCAVATED CRATERS IN CLAY



CHARGE DEPTH = 1.0 λ



CHARGE DEPTH = 1.0 λ



CHARGE DEPTH = 0.6 λ

FIGURE 20 - EXCAVATED CRATERS IN CLAY



CHARGE DEPTH = 0.6 λ

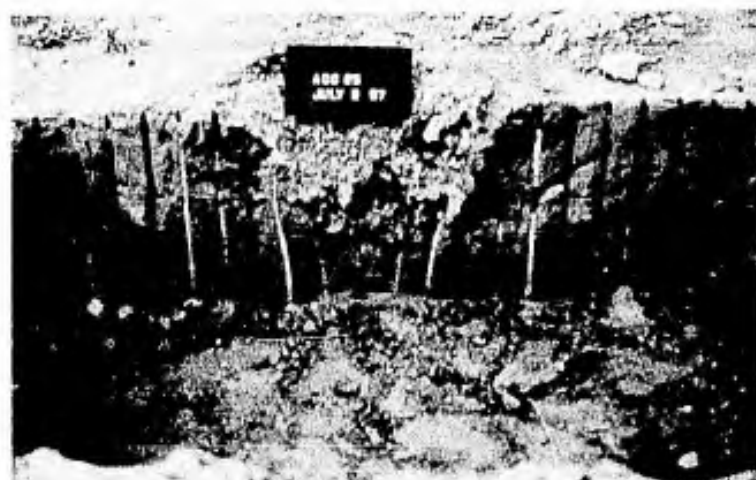


CHARGE DEPTH = 0.6 λ

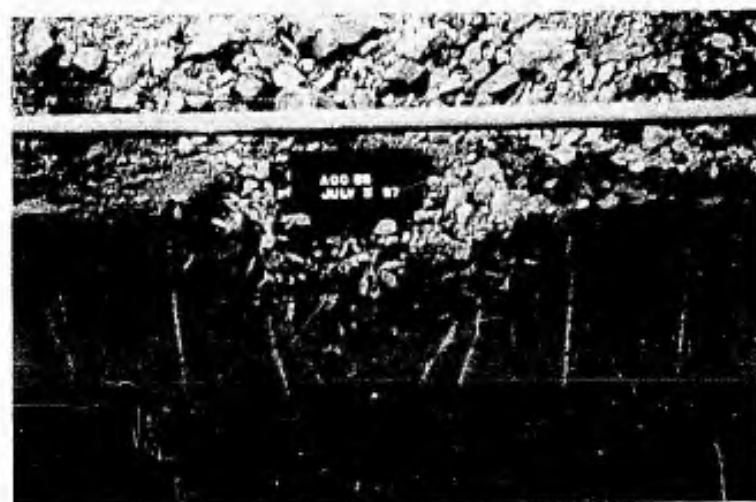


CHARGE DEPTH = 0.6 λ

FIGURE 21- EXCAVATED CRATERS IN CLAY



CHARGE DEPTH = 0.6λ



CHARGE DEPTH = 0.6λ



CHARGE DEPTH = 0.4λ

FIGURE 22—EXCAVATED CRATERS IN CLAY



CHARGE DEPTH = 0.4 λ



CHARGE DEPTH = 0.2 λ



CHARGE DEPTH = 0.2 λ

FIGURE 23-EXCAVATED CRATERS IN CLAY

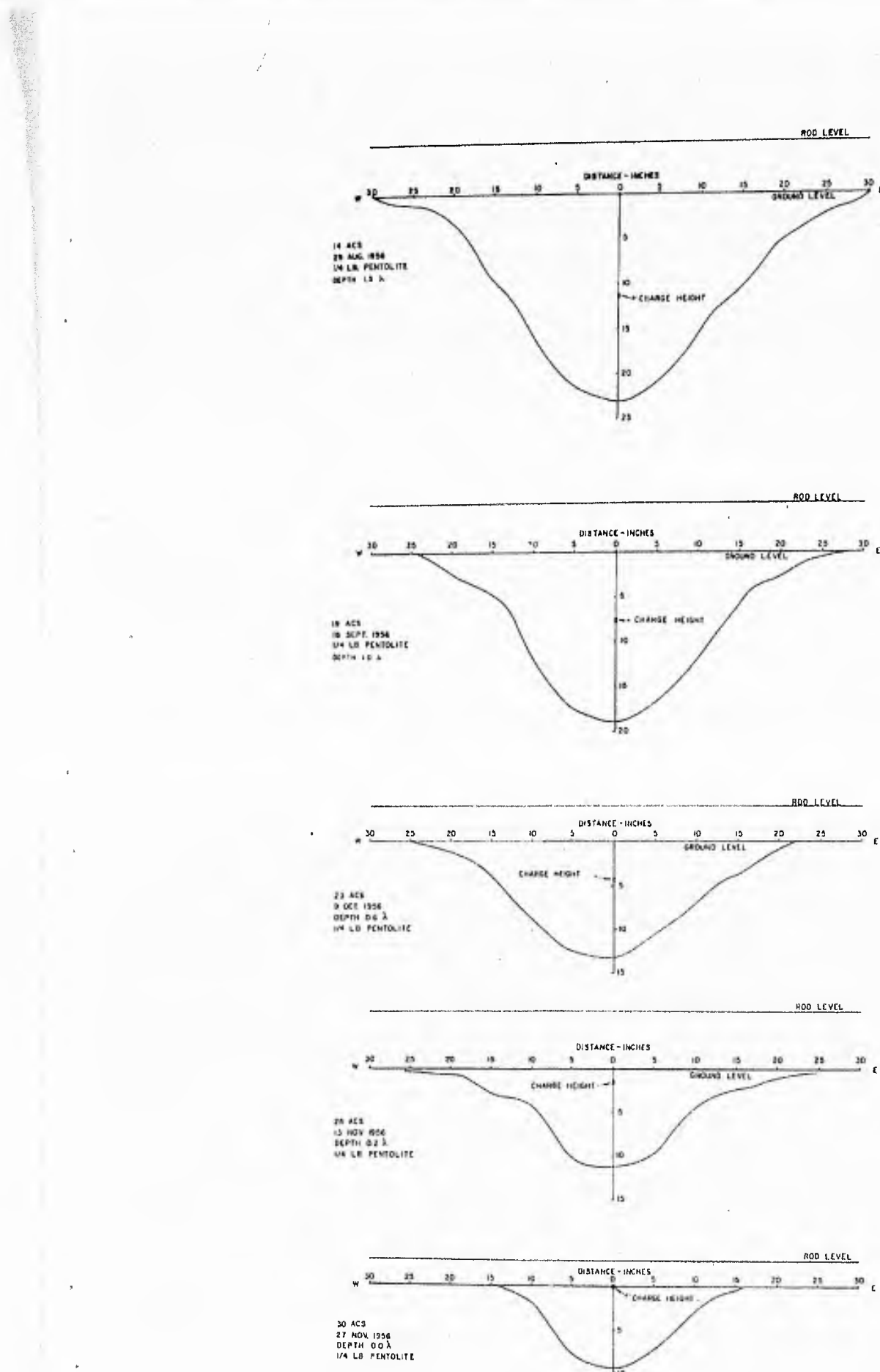


FIGURE 24. TYPICAL TRUE CRATER PROFILES IN SAND FOR SHOTS FROM 0 TO 15 SHOT DEPTH (SCALE RADII)

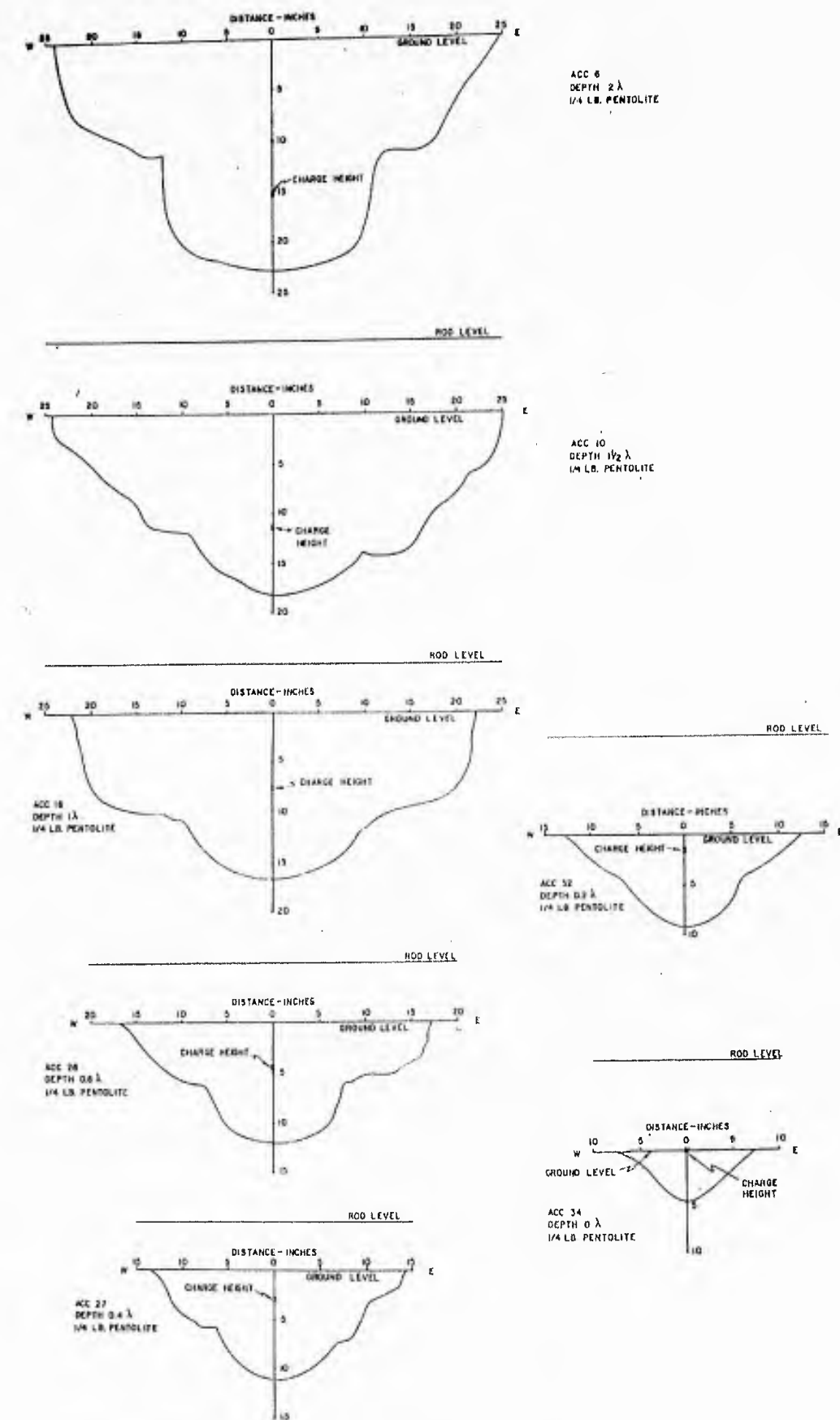


FIGURE 26. TYPICAL TRUE CRATER PROFILES IN CLAY FOR SHOTS FROM .0 TO 1.8 SHOT DEPTH (SCALE RADII)

APPENDIX C

ACCELERATIONS VS TIMES

1. Accelerations vs Times in Sand
2. Accelerations vs Times in Clay

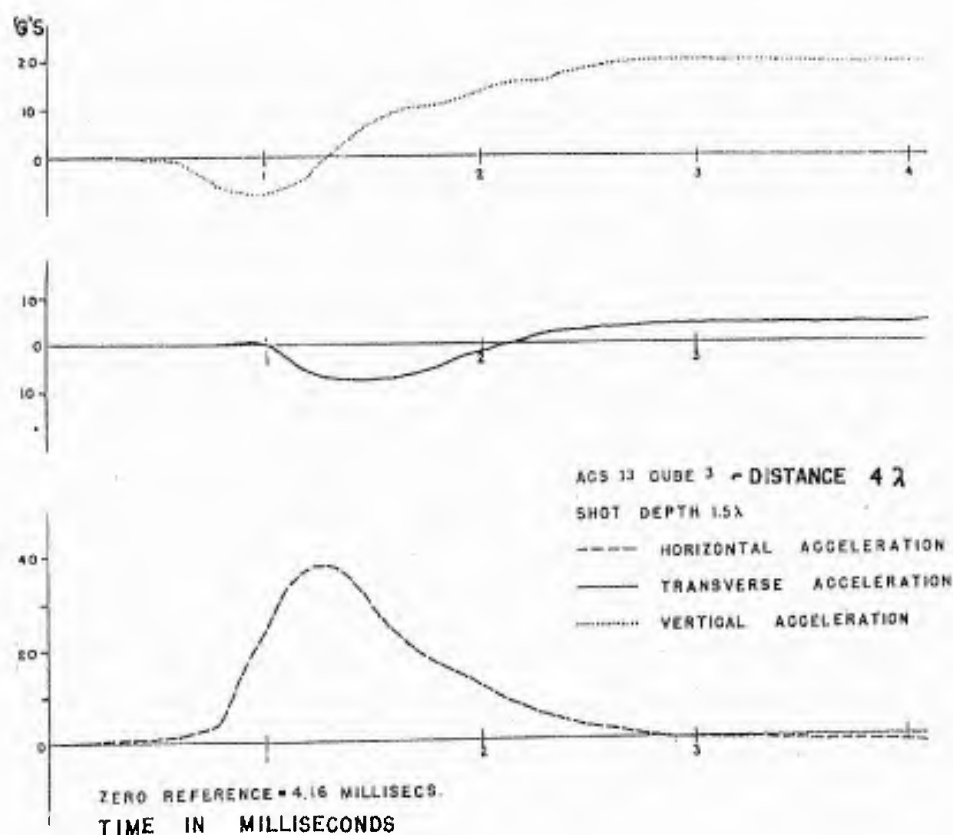
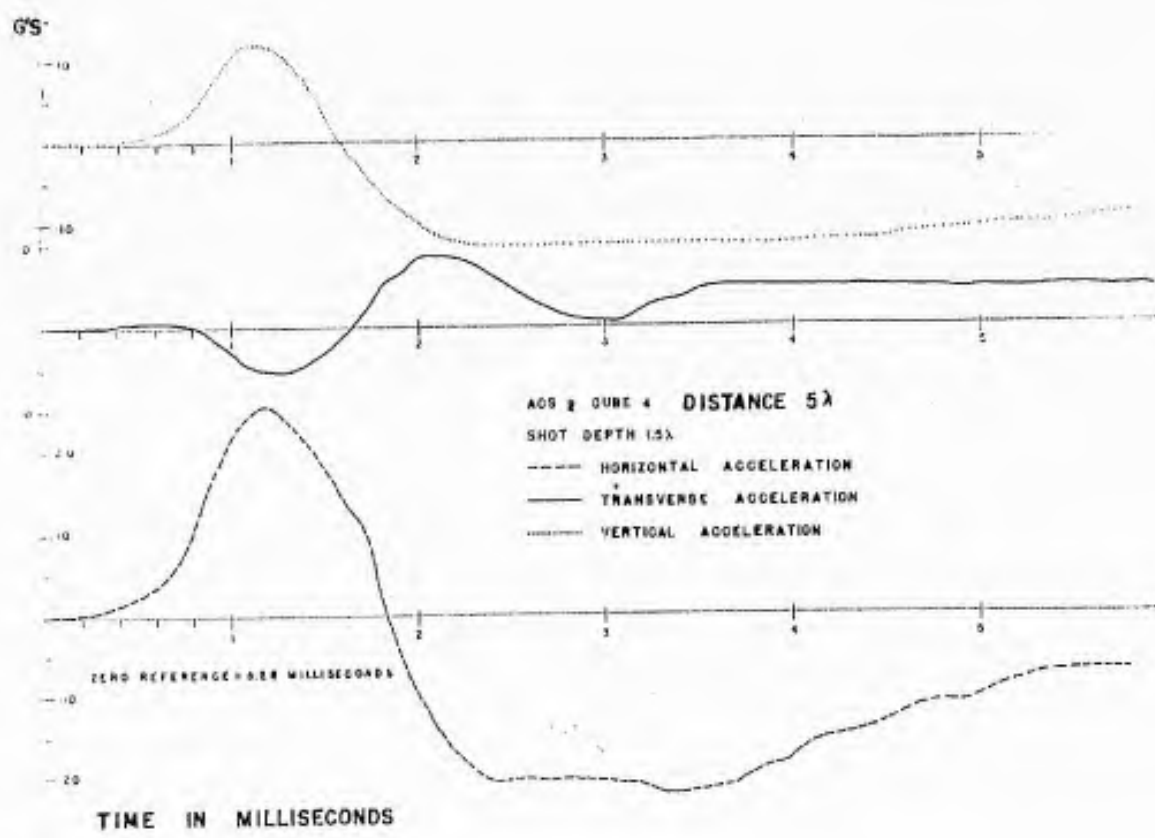


FIGURE 26 - ACCELERATIONS vs. TIMES IN SAND

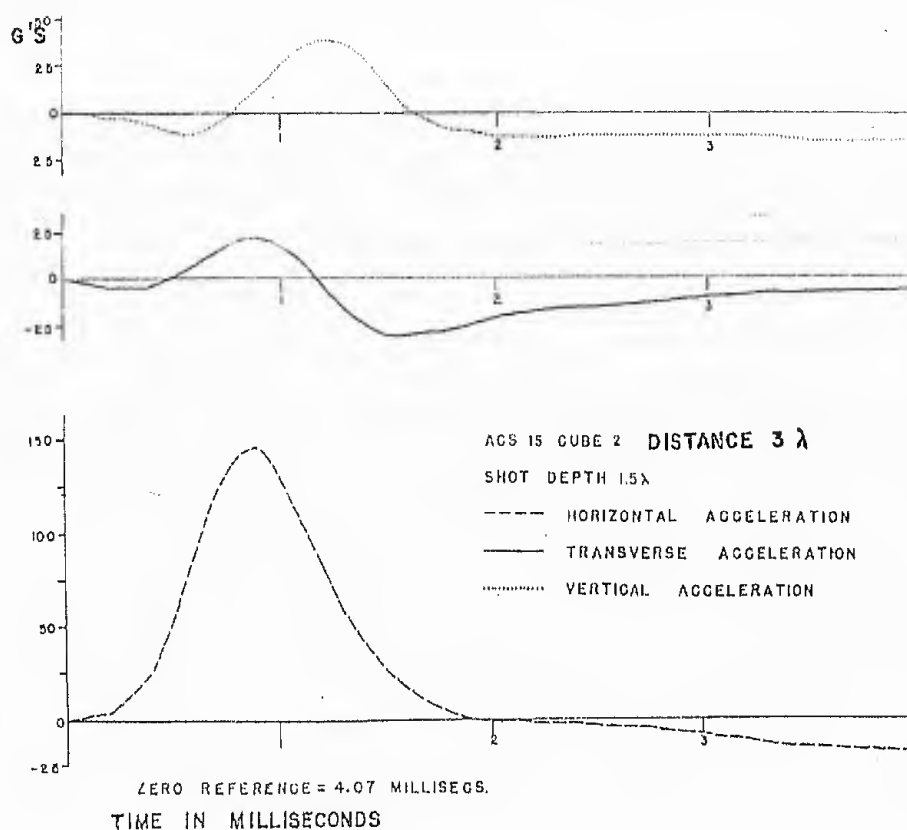
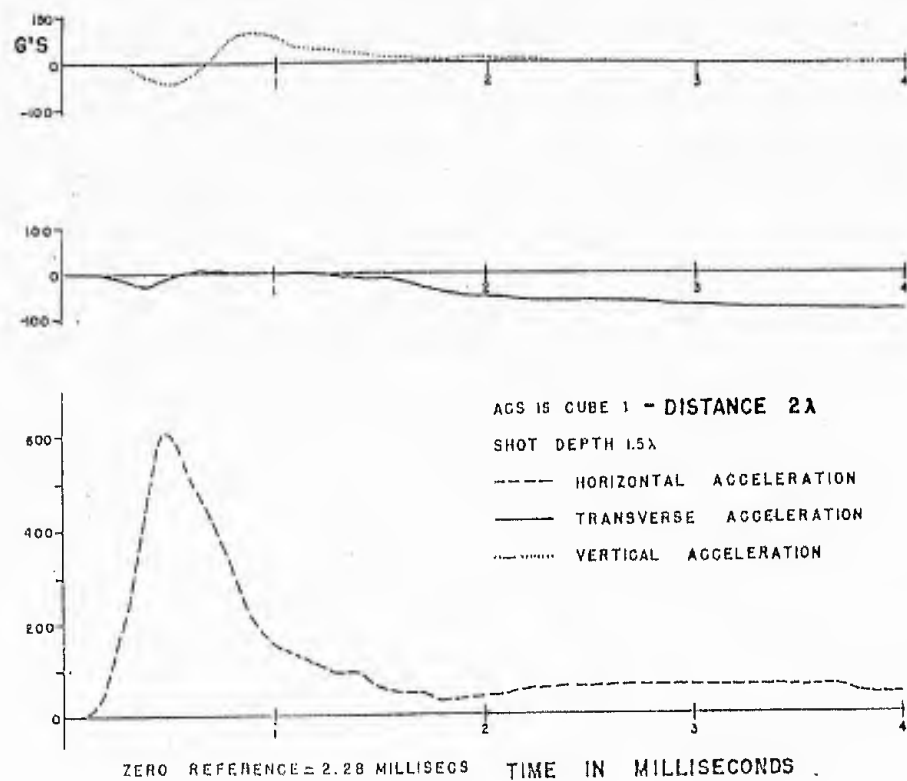


FIGURE 27-ACCELERATIONS vs. TIMES IN SAND

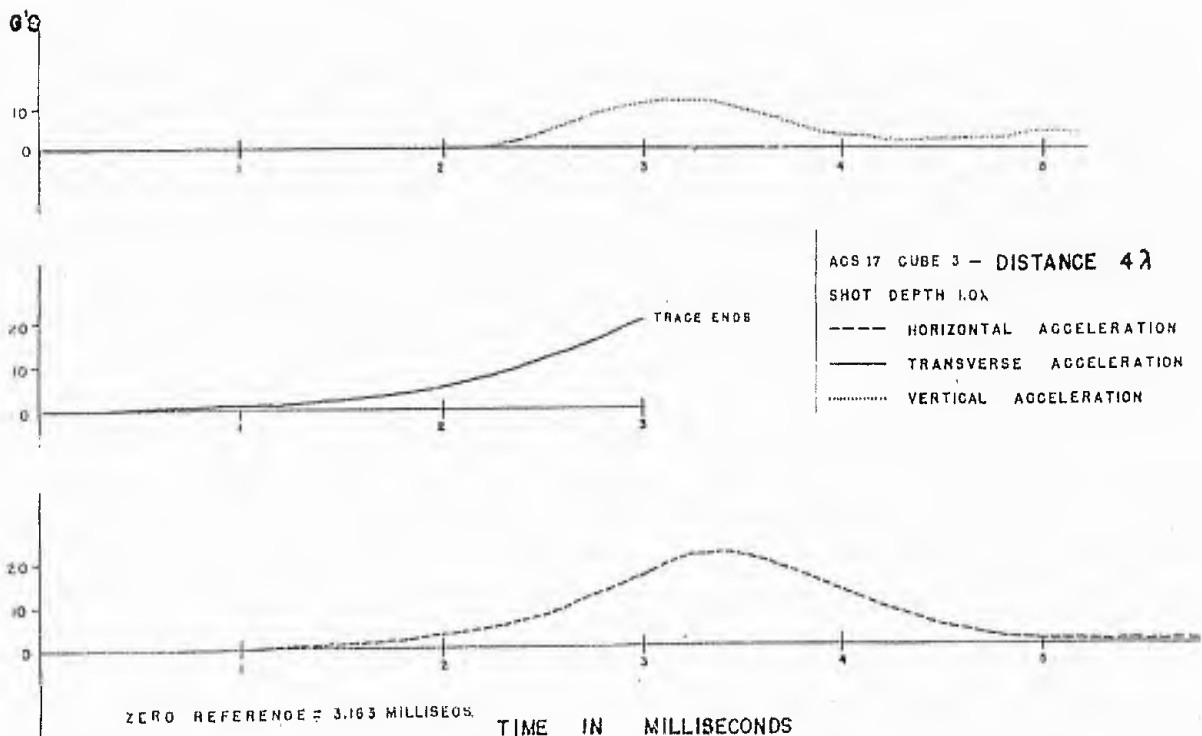
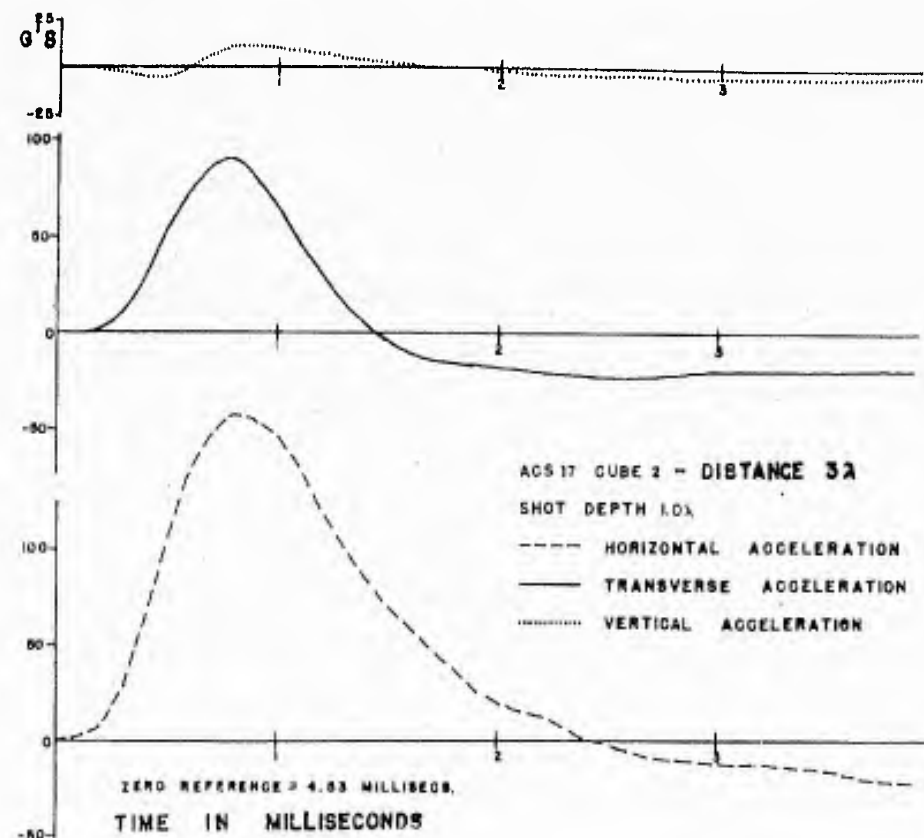


FIGURE 28- ACCELERATIONS vs. TIMES IN SAND

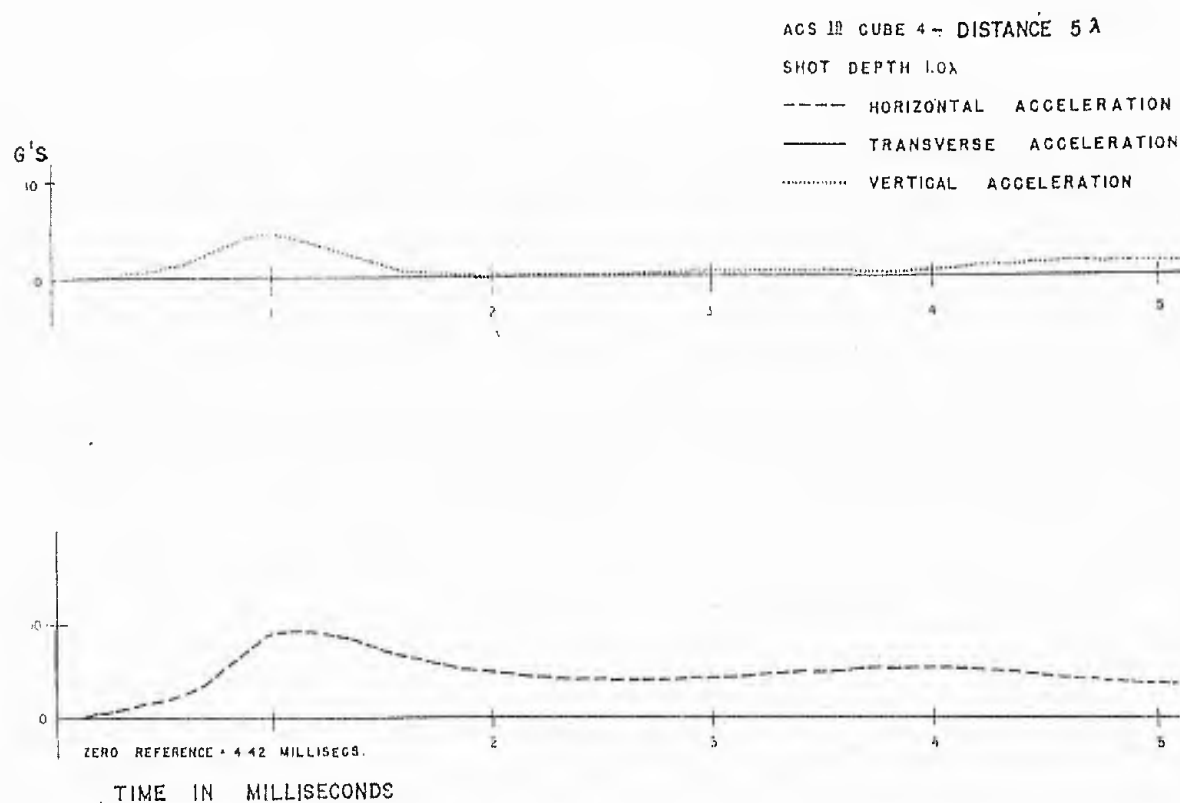
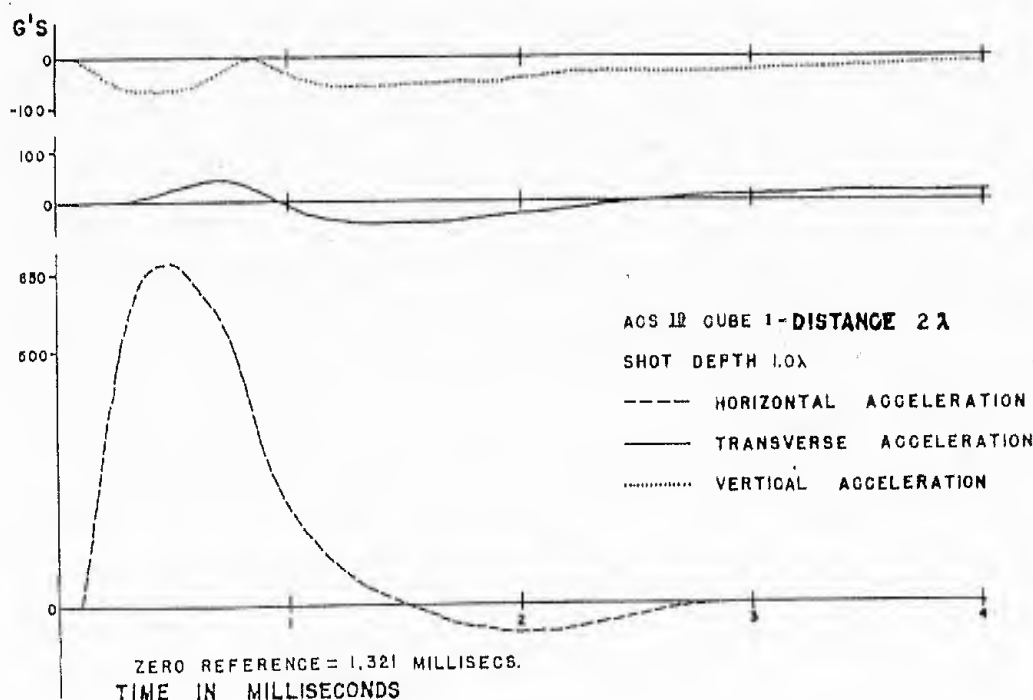


FIGURE 29-ACCELERATIONS vs. TIMES IN SAND

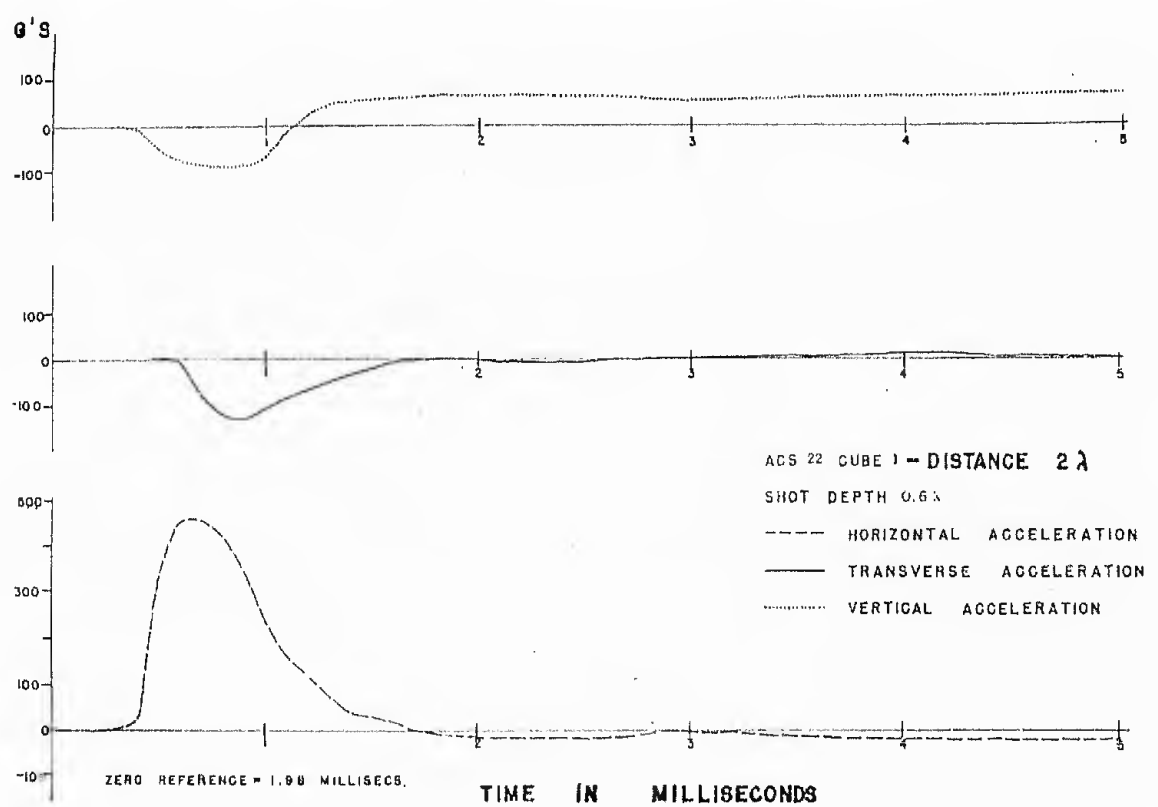
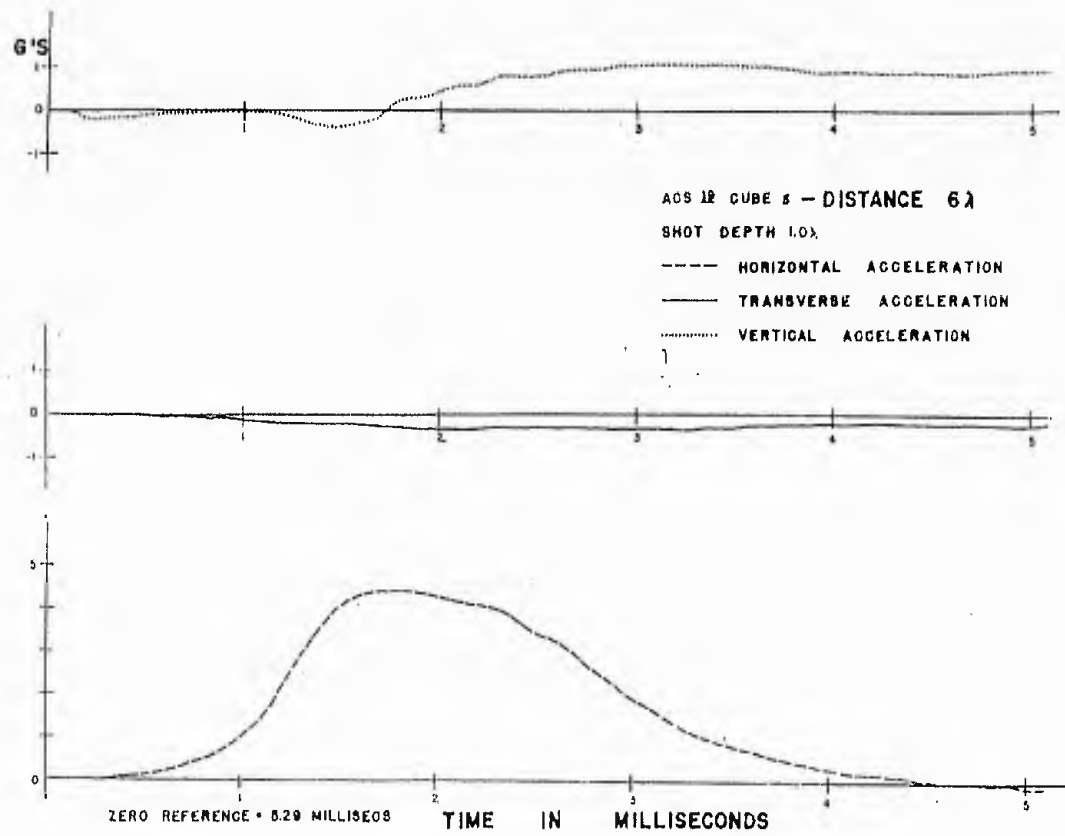


FIGURE 30 - ACCELERATIONS vs. TIMES IN SAND

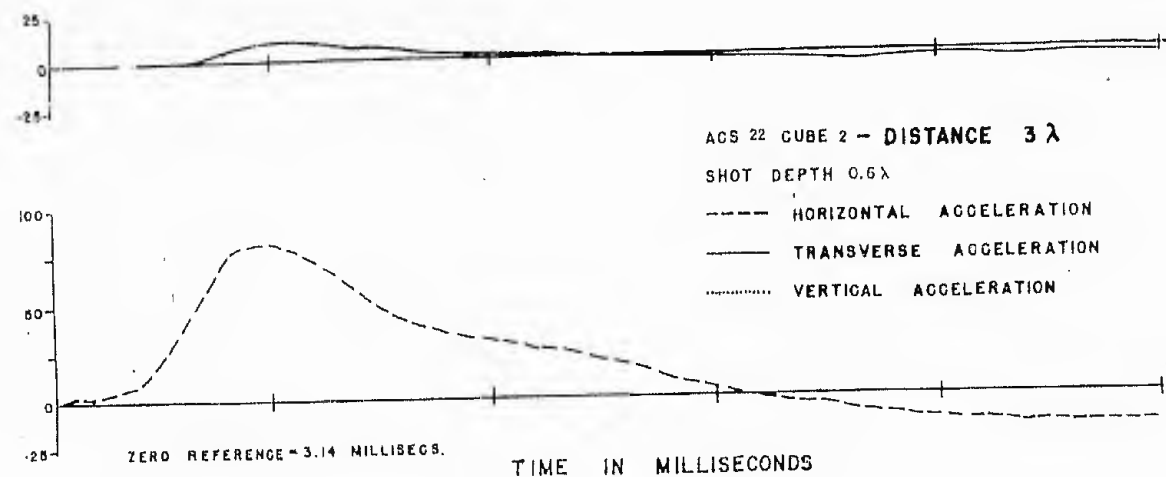
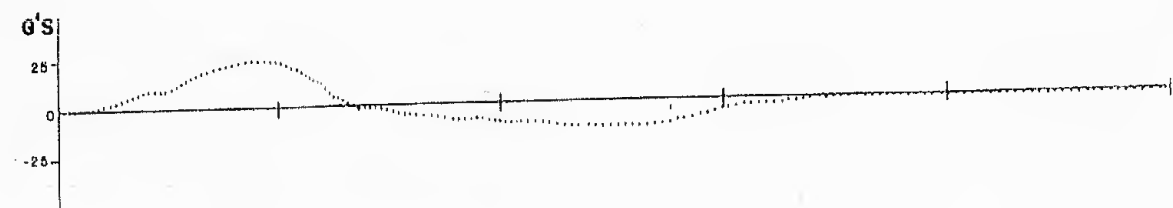


FIGURE 31-ACCELERATIONS vs. TIMES IN SAND

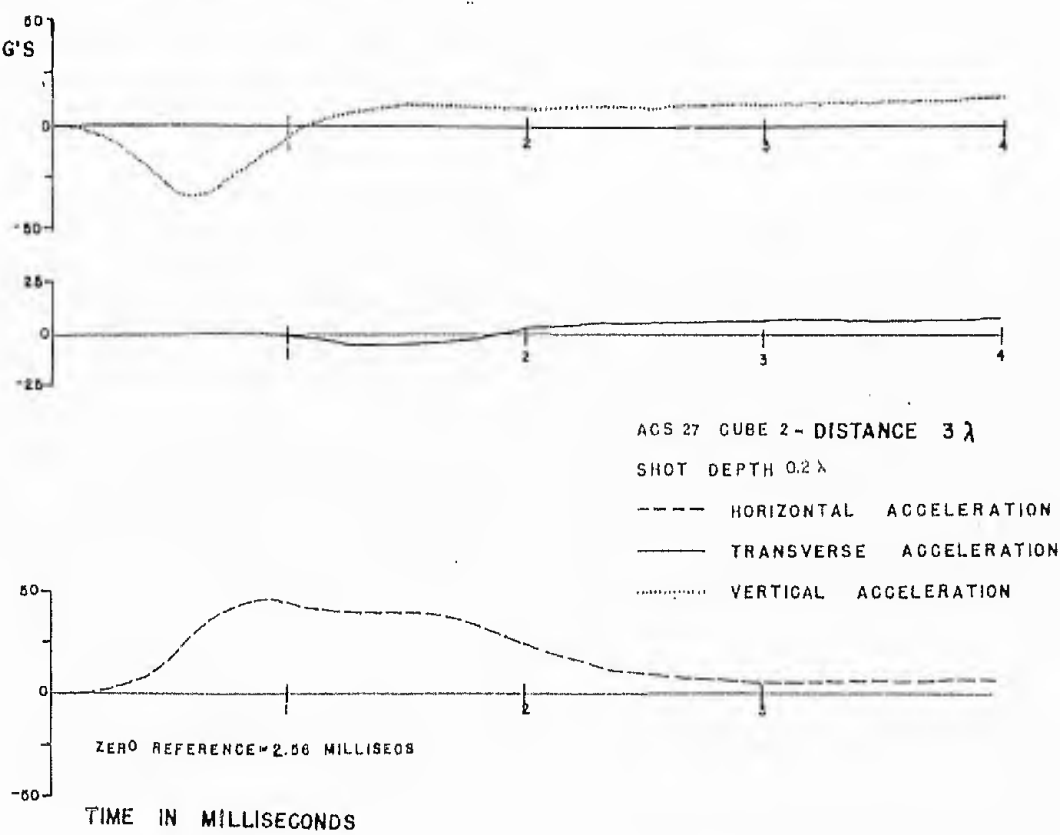
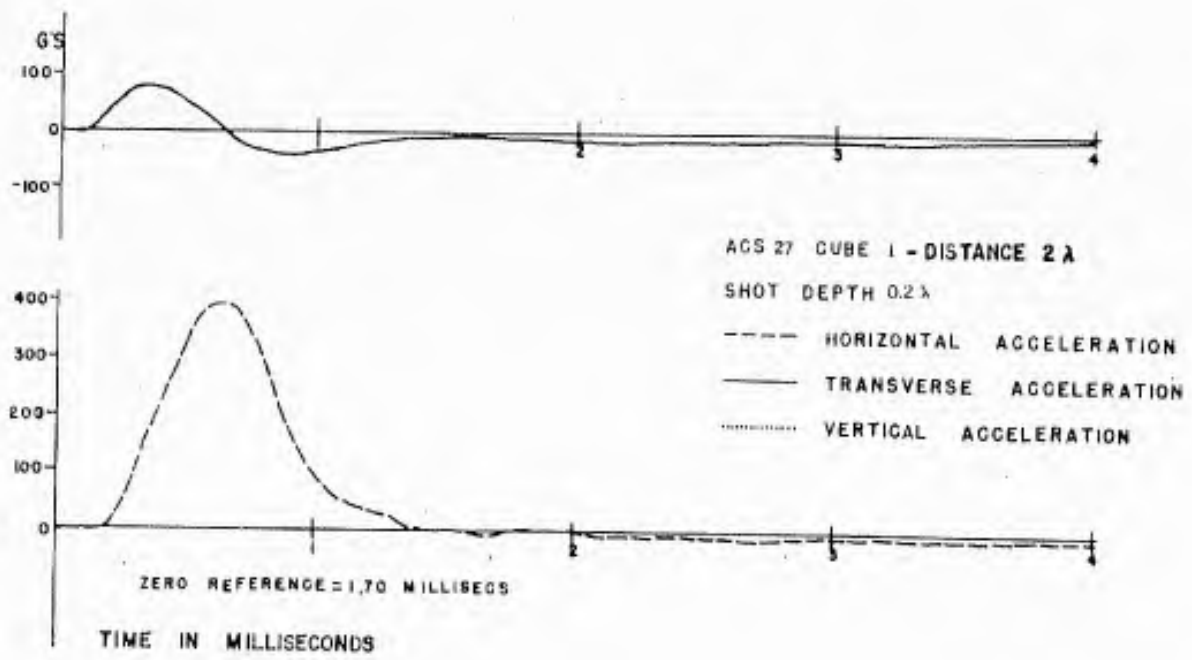


FIGURE 32-ACCELERATIONS vs. TIMES IN SAND

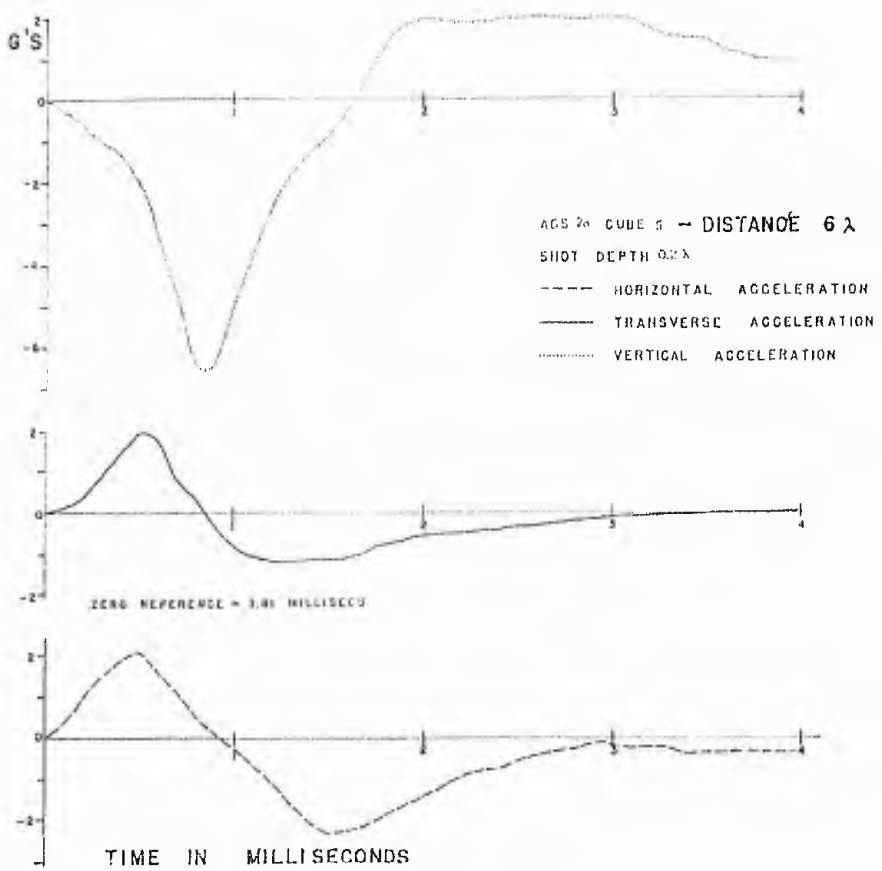
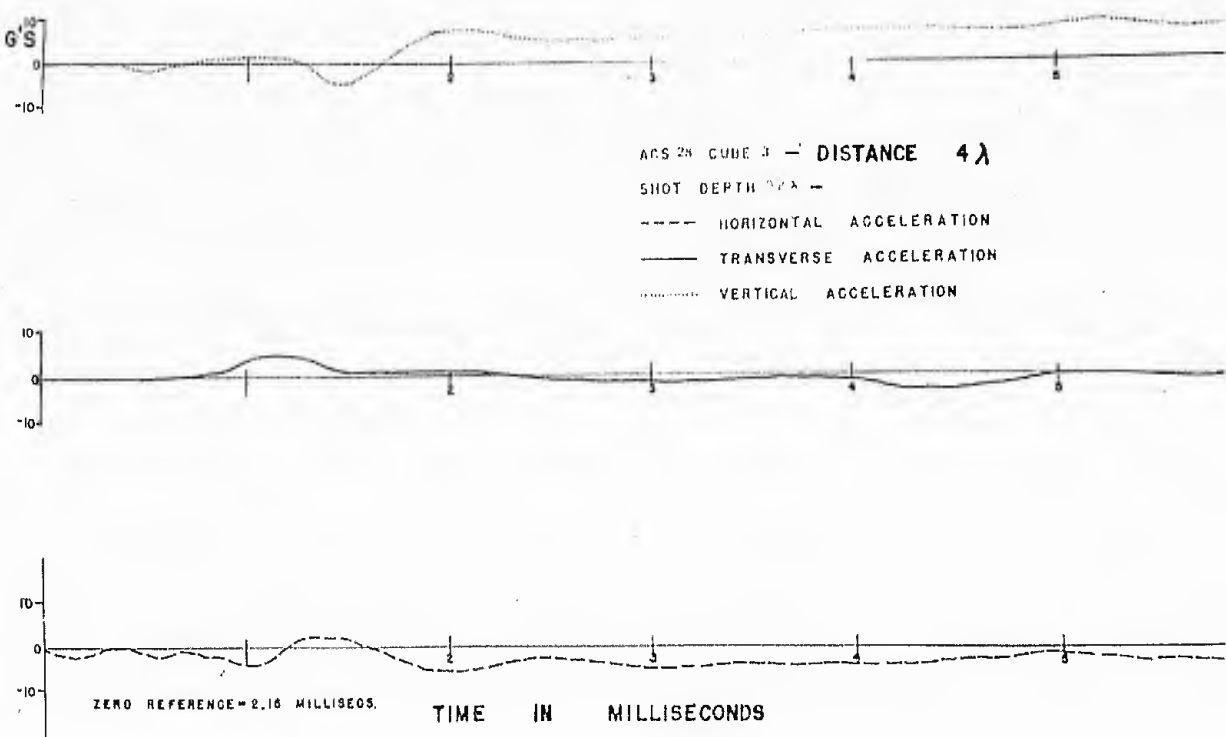


FIGURE 33-ACCELERATIONS vs. TIMES IN SAND

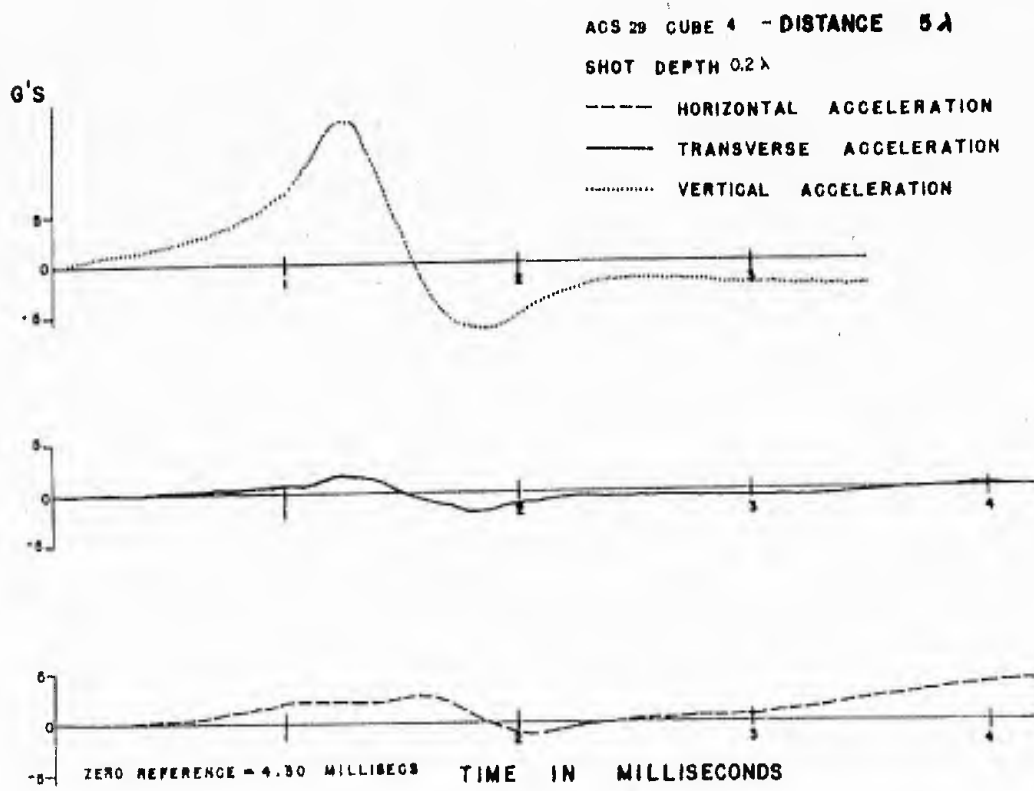


FIGURE 34-ACCELERATIONS VS. TIMES IN SAND

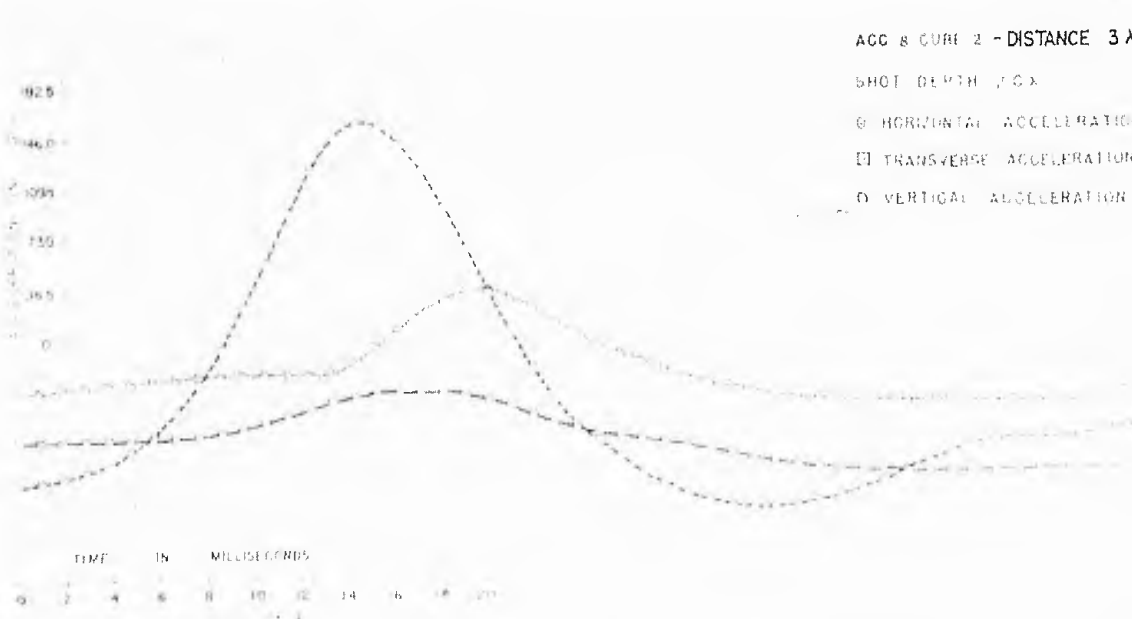
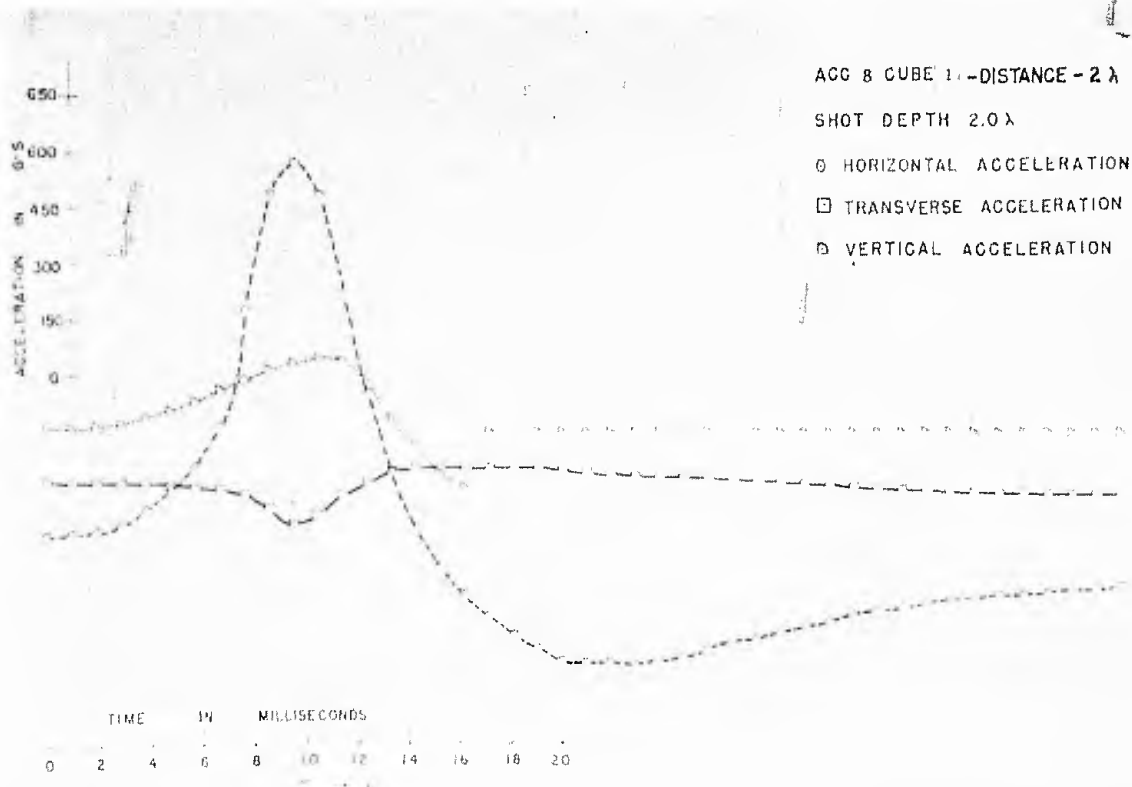


FIGURE 35 - ACCELERATIONS vs. TIMES IN CLAY

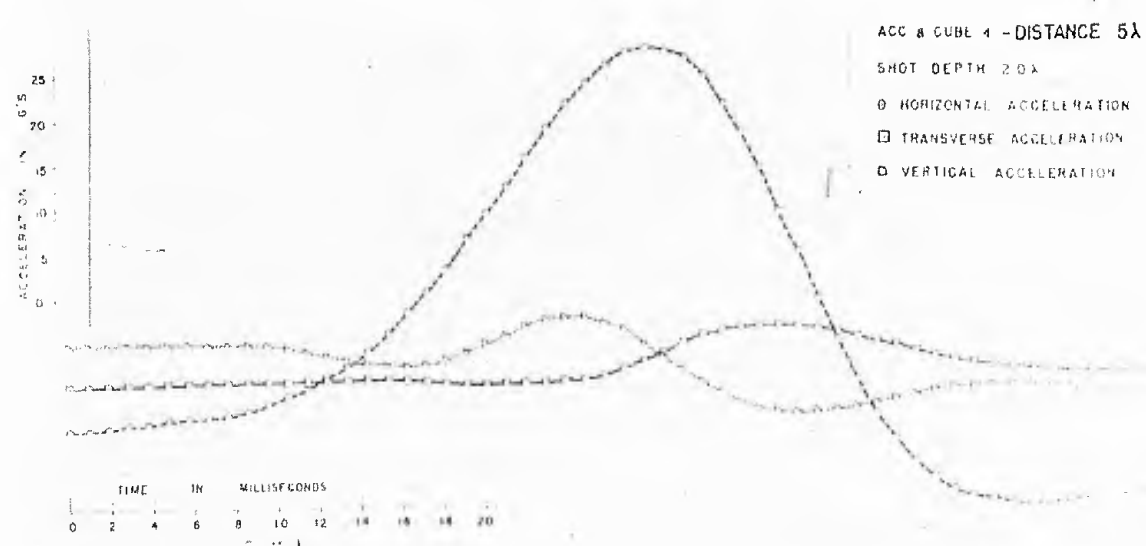
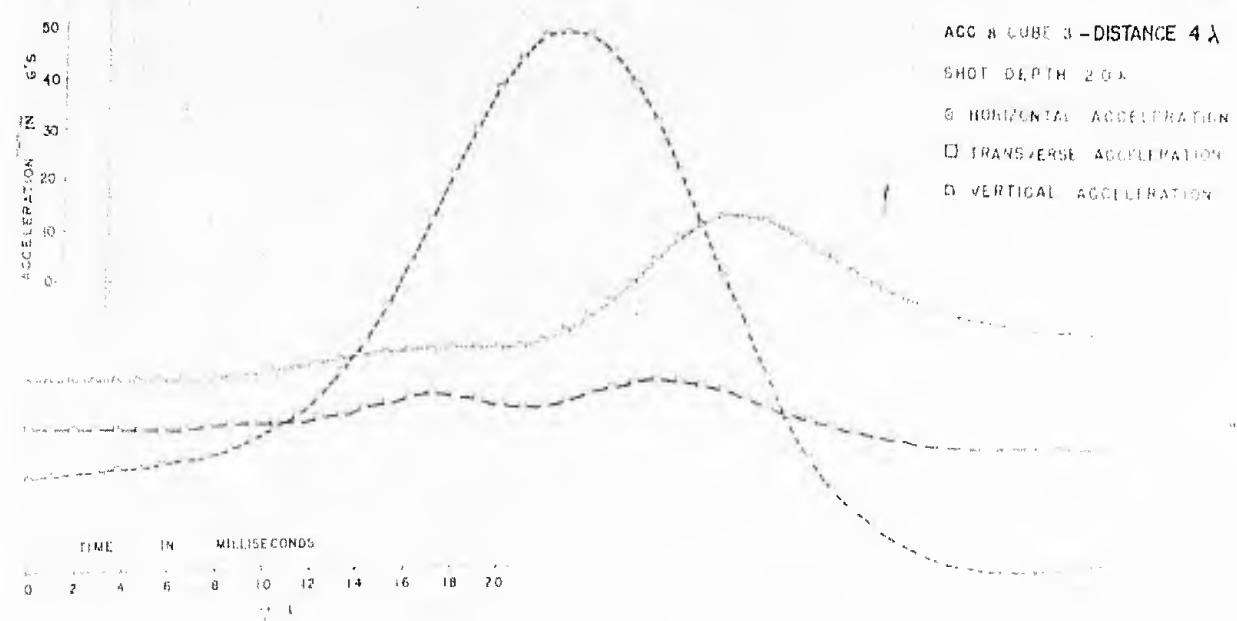


FIGURE 36-ACCELERATIONS vs. TIMES IN CLAY

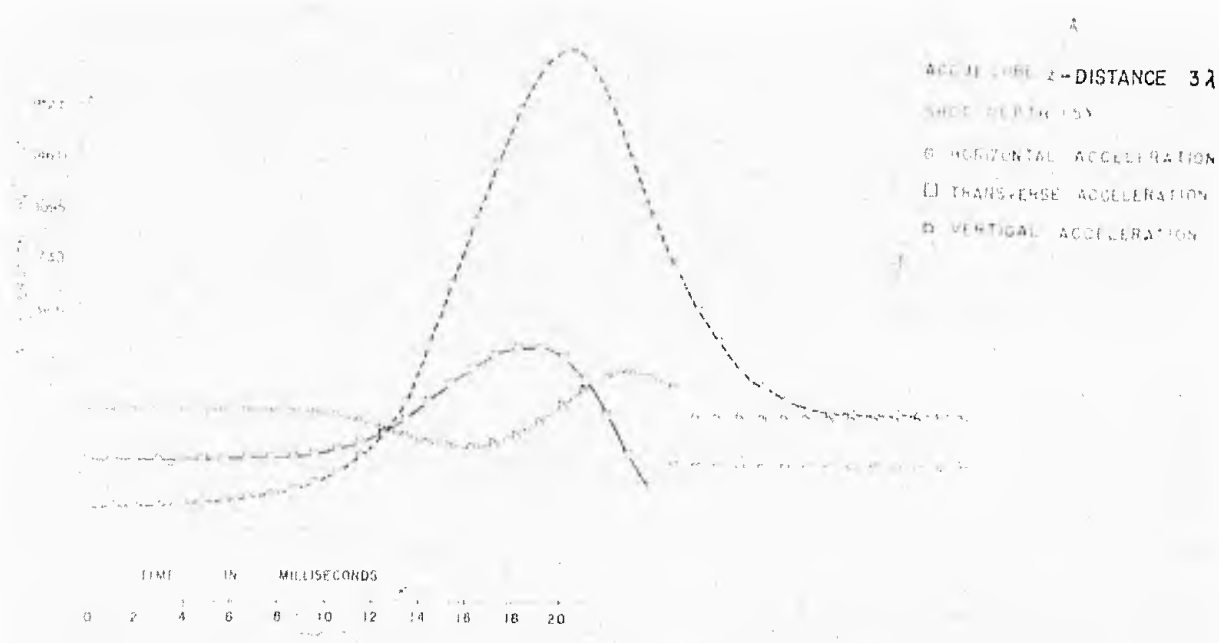
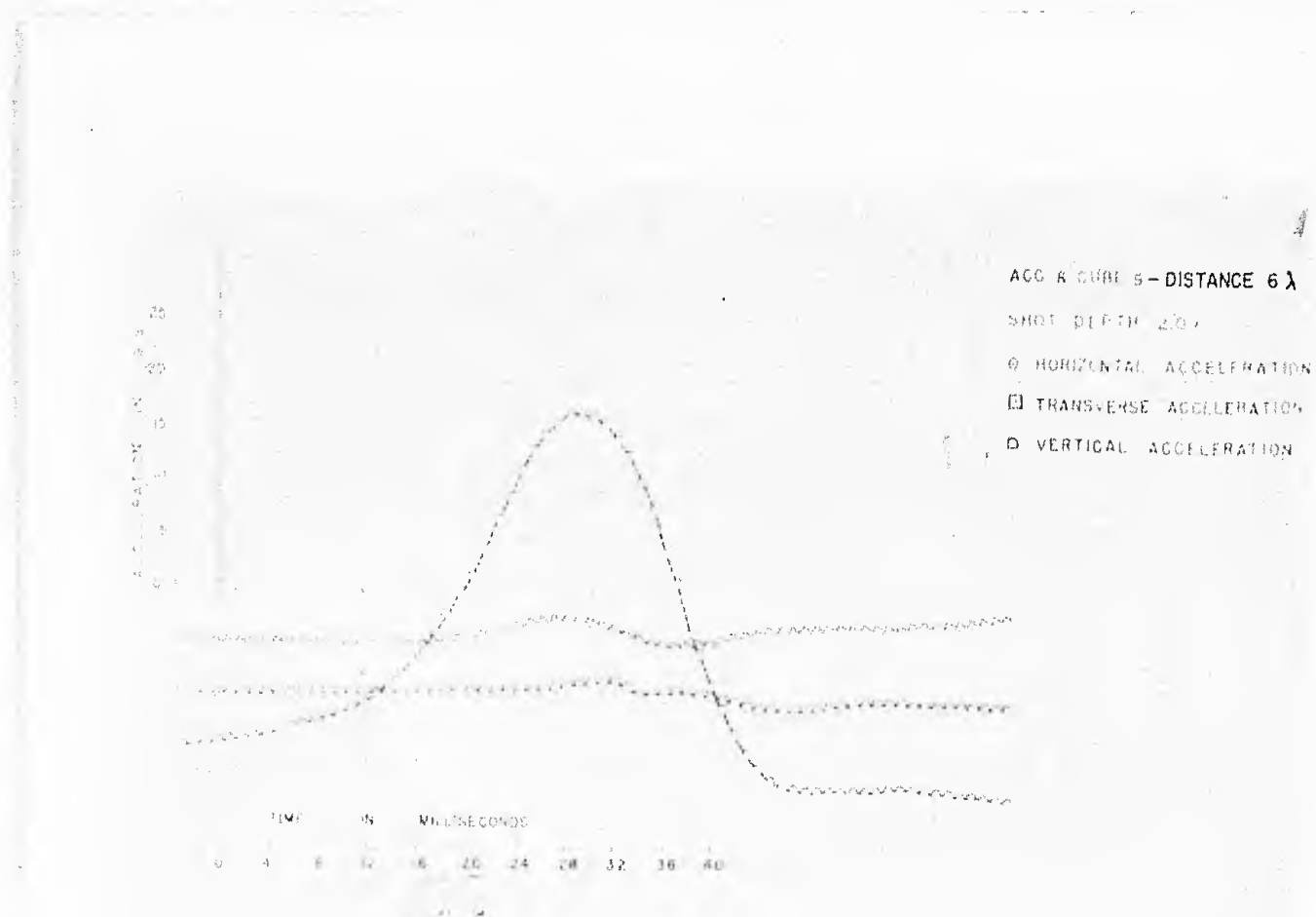


FIGURE 37 - ACCELERATIONS vs. TIMES IN CLAY

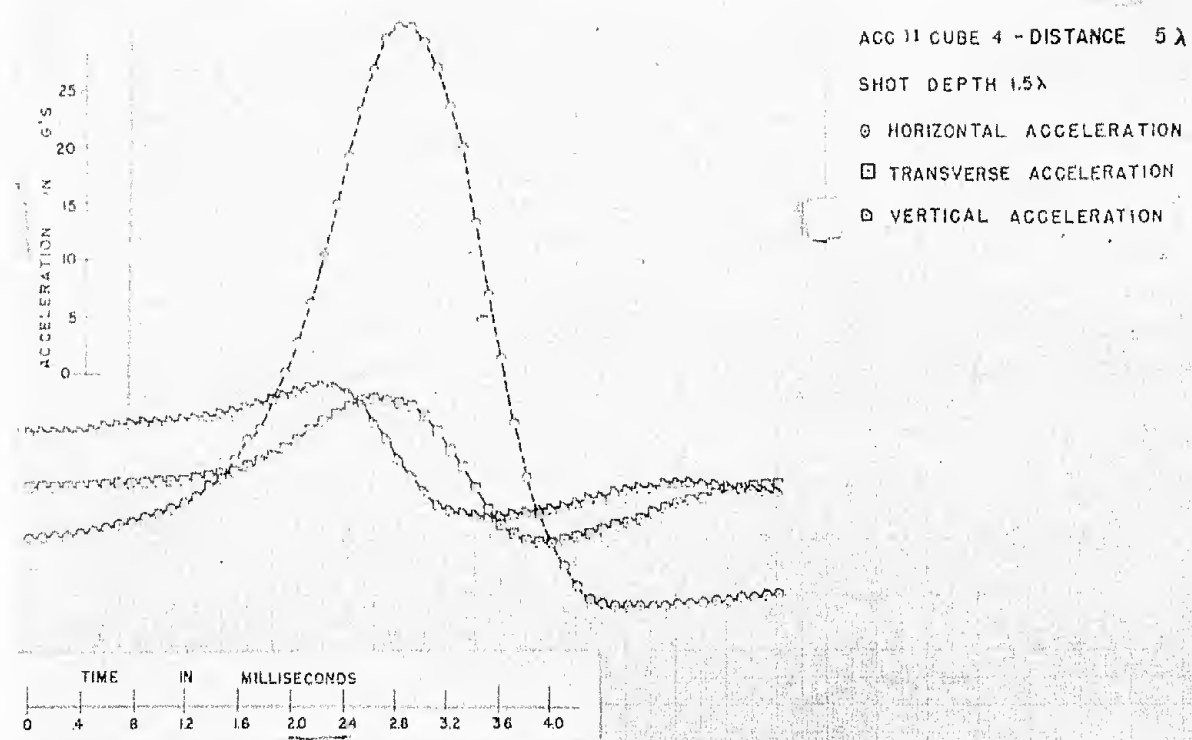
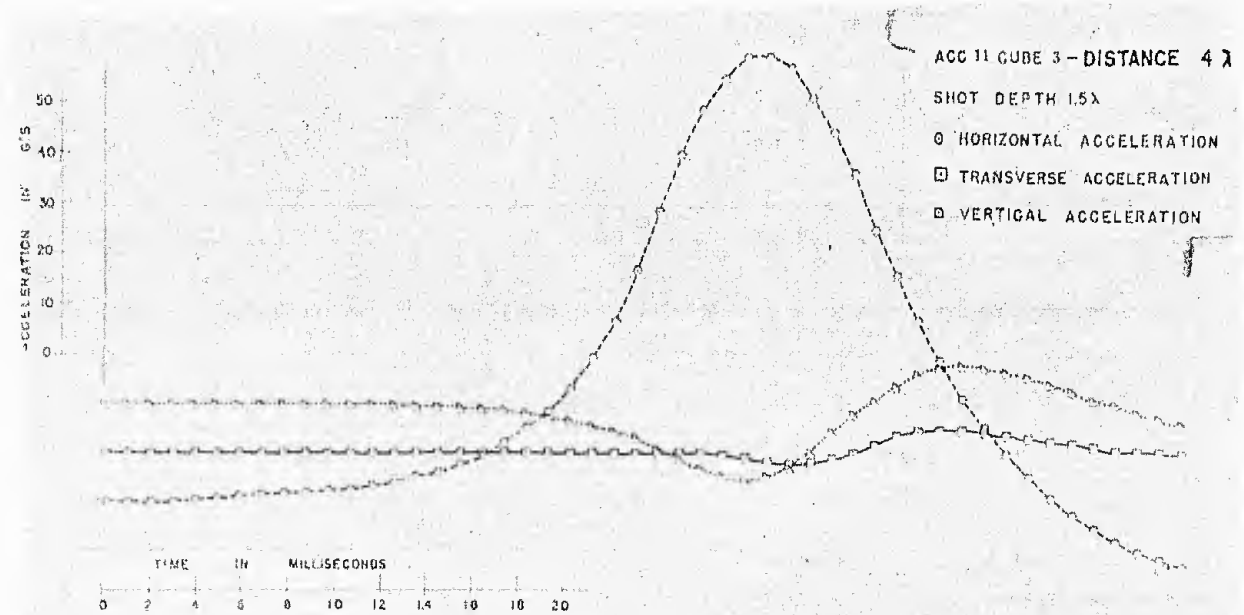


FIGURE 38 - ACCELERATIONS vs. TIMES IN CLAY

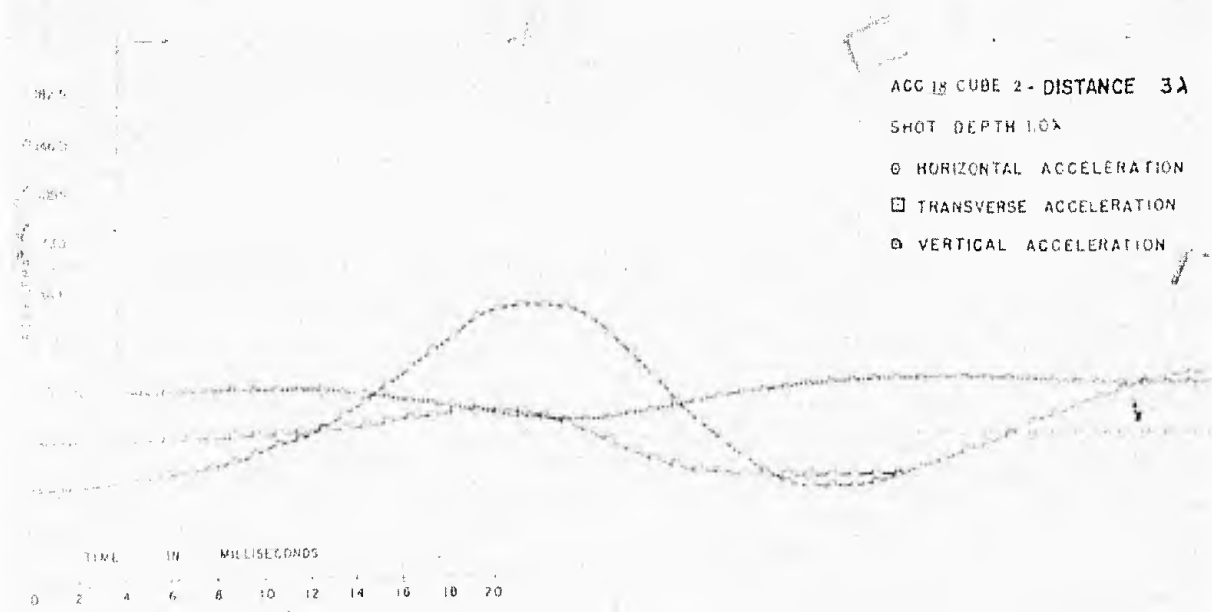
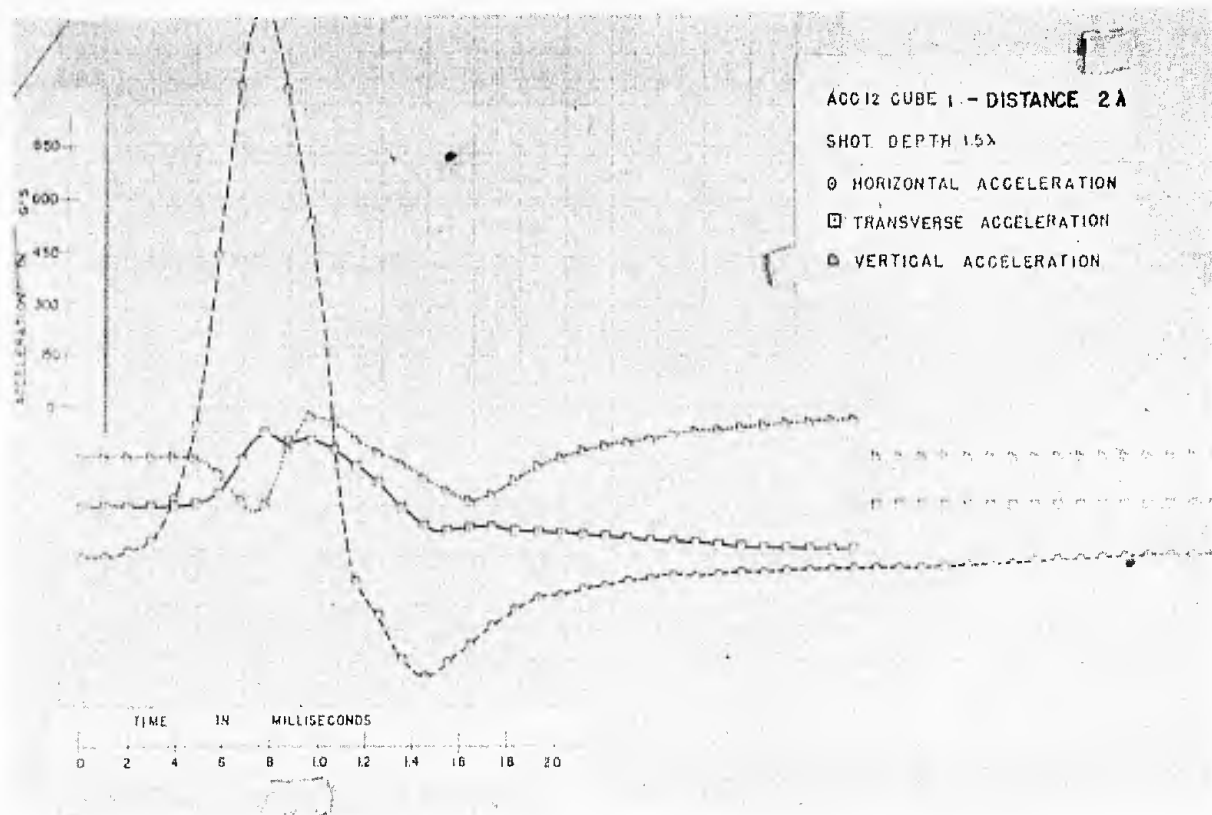


FIGURE 39-ACCELERATIONS vs. TIMES IN CLAY

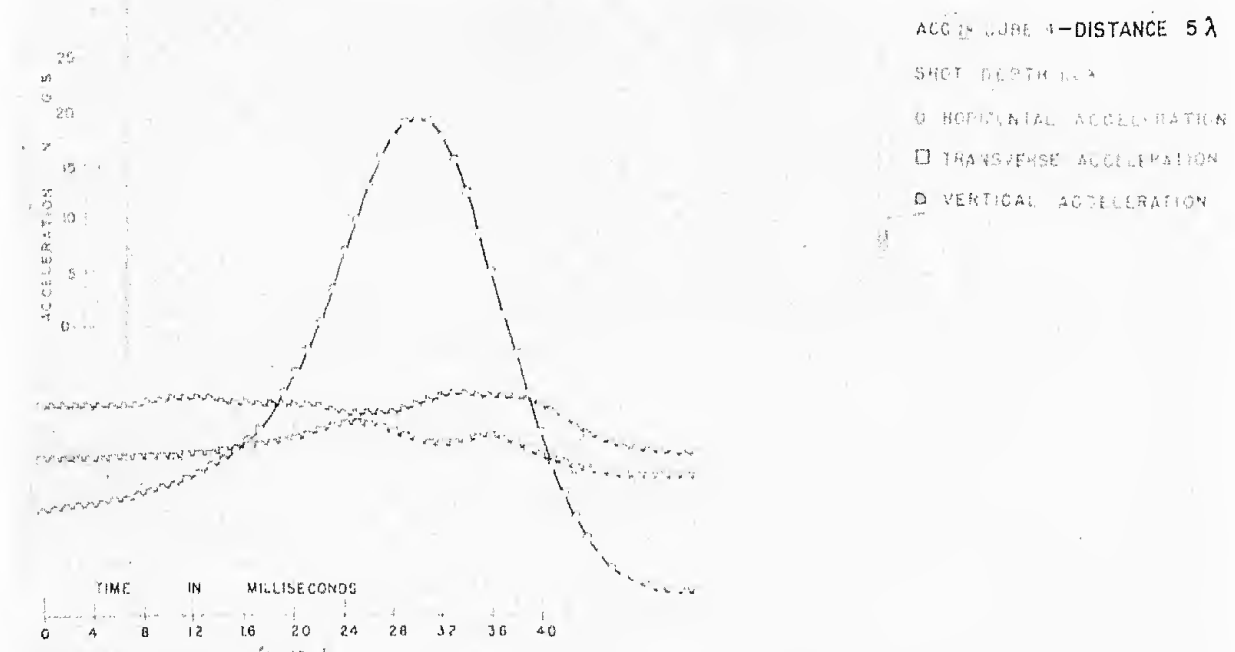
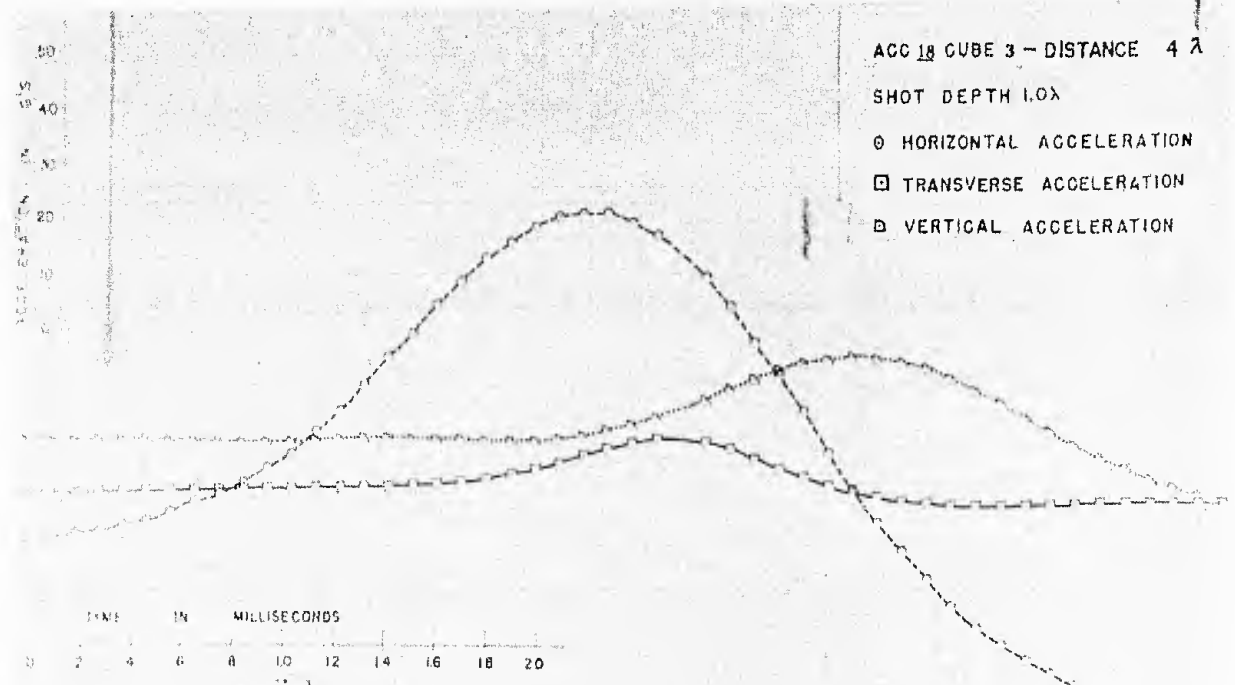


FIGURE 40-ACCELERATIONS vs. TIMES IN CLAY

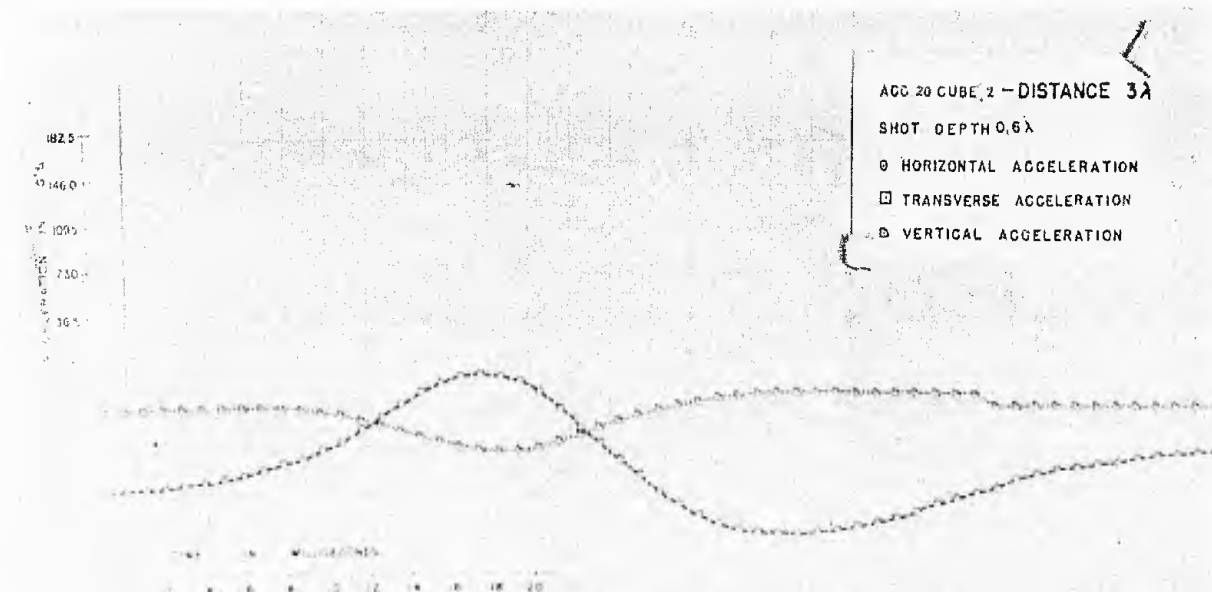
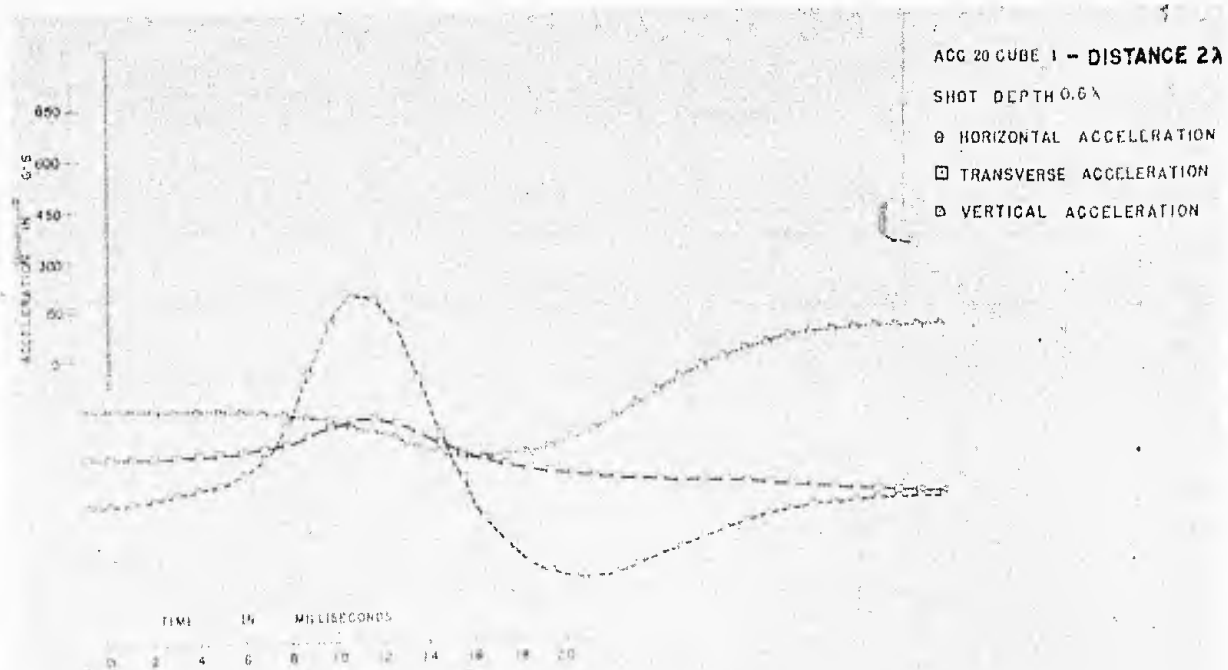


FIGURE 41 - ACCELERATIONS VS. TIMES IN CLAY

DISTRIBUTION LIST

<u>No. of Copies</u>	<u>Organization</u>	<u>No. of Copies</u>	<u>Organization</u>
10	Commander Armed Services Technical Information Agency ATTN: TIPCR Arlington Hall Station Arlington 12, Virginia	1	Commanding Officer Diamond Ordnance Fuze Laboratories ATTN: Technical Information Office, Branch 012 Washington 25, D. C.
5	Chief, Defense Atomic Support Agency ATTN: Mr. John Lewis Washington 25, D. C.	1	Research Analysis Corporation ATTN: Document Control Office 6935 Arlington Road Bethesda, Maryland Washington 14, D. C.
1	Commanding General Field Command Defense Atomic Support Agency Sandia Base P. O. Box 5100 Albuquerque, New Mexico	1	Commanding Officer U. S. Army Chemical Warfare Laboratories Army Chemical Center, Maryland
3	Chief of Ordnance ATTN: ORDTB - Bal Sec ORDTP-FR-2121-61 (2 cys) Department of the Army Washington 25, D. C.	2	Chief of Engineers ATTN: Mr. Martin Kirkpatrick Lt. Col. Russell Hutchinson Department of the Army Washington 25, D. C.
2	Commanding General Frankford Arsenal ATTN: Pitman-Dunn Laboratory Library Branch, 0270, Bldg 40 Philadelphia 37, Pennsylvania	2	Director Waterways Experiment Station ATTN: Mr. G. L. Arbuthnot Mr. William Flathau Vicksburg, Mississippi
1	Commanding Officer Picatinny Arsenal ATTN: Feltman Research and Engineering Laboratories Dover, New Jersey	1	Director Army Research Office ATTN: Geophysics Branch Arlington Hall Station Arlington, Virginia
1	Commanding Officer Watertown Arsenal ATTN: Laboratory Watertown 72, Massachusetts	1	Commanding Officer Army Research Office (Durham) Box CM, Duke Station Durham, North Carolina
		1	Commanding General Engineer Research and Development Laboratories ATTN: Dr. T. G. Walsh U. S. Army Fort Belvoir, Virginia

DISTRIBUTION LIST

<u>No. of Copies</u>	<u>Organization</u>	<u>No. of Copies</u>	<u>Organization</u>
3	Chief, Bureau of Naval Weapons ATTN: DIS-33 Department of the Navy Washington 25, D. C.	1	Commander U. S. Naval Weapons Laboratory Dahlgren, Virginia
1	Chief of Naval Operations ATTN: Op-36 Department of the Navy Washington 25, D. C.	1	Commander Air Force Systems Command Andrews Air Force Base Washington 25, D. C.
2	Chief of Naval Research ATTN: Code 118 Department of the Navy Washington 25, D. C.	4	Commander Ballistic Systems Division ATTN: George Young AF Unit Post Office Los Angeles 25, California
1	Chief, Bureau of Yards & Docks ATTN: Cmdr. W.J. Christensen Department of the Navy Washington 25, D. C.	1	Commander Air Proving Ground Center ATTN: PGAPI Eglin Air Force Base, Florida
1	Commanding Officer & Director David W. Taylor Model Basin ATTN: Structural Mechanics Division Washington 7, D. C.	1	Commander Air Force Cambridge Research Laboratory ATTN: Geophysical Research Library L. G. Hanscom Field Bedford, Massachusetts
2	Commander Naval Ordnance Laboratory ATTN: Explosives Division White Oak, Silver Spring 19, Maryland	1	Commander Air Force Special Weapons Center ATTN: Research & Development- Colonel Huie Kirtland Air Force Base, New Mexico
1	Commanding Officer & Director U. S. Naval Civil Engineering Laboratory ATTN: Mr. J. Algood Port Hueneme, California	1	Director Air University Library ATTN: AUL (3T-AUL-60-118) Maxwell Air Force Base, Alabama
1	Commander U. S. Naval Ordnance Test Station ATTN: Technical Library China Lake, California	1	Deputy Chief of Staff for Operations ATTN: Assistant for Atomic Energy, AFQAT U. S. Air Force Washington 25, D. C.
2	Director U. S. Naval Research Laboratory Washington 25, D. C.		

DISTRIBUTION LIST

<u>No. of Copies</u>	<u>Organization</u>	<u>No. of Copies</u>	<u>Organization</u>
1	Deputy Chief of Staff, Development Director of Research & Development ATTN: Chief, Research Division U. S. Air Force Washington 25, D. C.	1	Armour Research Foundation Illinois Institute of Technology Center ATTN: Dr. T. H. Schiffman Chicago 16, Illinois
1	Chief, Bureau of Mines Washington 25, D. C.	1	The RAND Corporation ATTN: Dr. Brode 1700 Main Street Santa Monica, California
1	U.S. Atomic Energy Commission ATTN: Technical Reports Library Mrs. J. O'Leary for Division of Military Application Washington 25, D. C.	1	Applied Physics Laboratory The Johns Hopkins University 8621 Georgia Avenue Silver Spring, Maryland
2	U. S. Atomic Energy Commission Los Alamos Scientific Laboratory ATTN: Dr. Fred Reines P. O. Box 1663 Los Alamos, New Mexico	1	Stanford Research Institute ATTN: Mr. F. Sauer Menlo Park, California
1	U. S. Atomic Energy Commission Sandia Corporation ATTN: Physics Division - Mr. W. R. Perret P. O. Box 5800 Albuquerque, New Mexico	1	Professor Walker Bleakney Palmer Physical Laboratory Princeton, New Jersey
1	Executive Secretary Military Liaison Committee to The Atomic Energy Commission 1901 Constitution Avenue, N.W. Washington, D.C.	1	Mr. Kenneth Kaplan Broadview Research Corporation 1811 Trousdale Drive Burlingame, California
1	University of California Lawrence Radiation Laboratory Technical Information Division ATTN: Clovis G. Craig P. O. Box 808 Livermore, California Of Interest to: Dr. R. G. Preston	1	Dr. Otto LaPorte Engineering Research Institute University of Michigan Ann Arbor, Michigan
		1	Dr. N. M. Newmark 111 Talbot Laboratory University of Illinois Urbana, Illinois
		1	Dr. Leonard Obert Applied Physics Division U. S. Bureau of Mines College Park 1, Maryland

DISTRIBUTION LIST

<u>No. of</u>	<u>Copies</u>	<u>Organization</u>
1		Professor J. Neils Thompson Civil Engineering Department University of Texas Austin 12, Texas
1		Dr. Robert V. Whitman Massachusetts Institute of Technology Cambridge 39, Massachusetts
10		Commander British Army Staff British Defence Staff (W) ATTN: Reports Officer 3100 Massachusetts Avenue, N.W. Washington 8, D. C.
4		Defence Research Member Canadian Joint Staff 2450 Massachusetts Avenue, N.W. Washington 8, D. C.

<p>AD Ballistic Research Laboratories, ARS MECHANICS OF CRATER FORMATION IN SAND AND CLAY PRODUCED BY UNDERGROUND EXPLOSIONS W. H. Townsend, Mark Langseth and E. Perkins, Jr. ERL Memorandum Report No. 1361 December 1961 DA Proj. No. 503-04-002, ONSC No. 5010.11.815 UNCLASSIFIED Report</p>	<p>UNCLASSIFIED</p> <p>Accession No. AD Ballistic Research Laboratories, ARS MECHANICS OF CRATER FORMATION IN SAND AND CLAY PRODUCED BY UNDERGROUND EXPLOSIONS W. H. Townsend, Mark Langseth and E. Perkins, Jr. ERL Memorandum Report No. 1361 December 1961 DA Proj. No. 503-04-002, ONSC No. 5010.11.815 UNCLASSIFIED Report</p>	<p>Studies of crater dimensions versus shot depth have been made for sand and clay. By using a colored column technique, true crater dimensions and depths have been measured. Mineral and moisture content have been held nearly constant. Strength, grain size, soil density, cohesion and plasticity were measured. Accelerations of the ground particle versus distance were measured for shot depths ranging from zero to 2 units of scale distance. The values of the acceleration at a given distance from successive explosions at the same depth had an average deviation from the mean value of approximately 25 per cent for both sand and clay. The average deviation of the crater dimensions was less than 10 per cent from the mean for sand and less than 5 per cent for clay.</p>
<p>AD Ballistic Research Laboratories, ARS MECHANICS OF CRATER FORMATION IN SAND AND CLAY PRODUCED BY UNDERGROUND EXPLOSIONS W. H. Townsend, Mark Langseth and E. Perkins, Jr. ERL Memorandum Report No. 1361 December 1961 DA Proj. No. 503-04-002, ONSC No. 5010.11.815 UNCLASSIFIED Report</p>	<p>UNCLASSIFIED</p> <p>Accession No. AD Ballistic Research Laboratories, ARS MECHANICS OF CRATER FORMATION IN SAND AND CLAY PRODUCED BY UNDERGROUND EXPLOSIONS W. H. Townsend, Mark Langseth and E. Perkins, Jr. ERL Memorandum Report No. 1361 December 1961 DA Proj. No. 503-04-002, ONSC No. 5010.11.815 UNCLASSIFIED Report</p>	<p>Studies of crater dimensions versus shot depth have been made for sand and clay. By using a colored column technique, true crater dimensions and depths have been measured. Mineral and moisture content have been held nearly constant. Strength, grain size, soil density, cohesion and plasticity were measured. Accelerations of the ground particle versus distance were measured for shot depths ranging from zero to 2 units of scale distance. The values of the acceleration at a given distance from successive explosions at the same depth had an average deviation from the mean value of approximately 25 per cent for both sand and clay. The average deviation of the crater dimensions was less than 10 per cent from the mean for sand and less than 5 per cent for clay.</p>

<p>AD Ballistic Research Laboratories, ARG MECHANICS OF CRATER FORMATION IN SAND AND CLAY PRODUCED BY UNDERGROUND EXPLOSIONS W. E. Townsend, Mark Langseth and B. Perkins, Jr. ERL Memorandum Report No. 1381 December 1961 DA Proj. No. 503-01-002, OMSC No. 5010-11-814 UNCLASSIFIED Report</p>	<p>UNCLASSIFIED</p>	<p>Accession No. Ballistic Research Laboratories, ARG MECHANICS OF CRATER FORMATION IN SAND AND CLAY PRODUCED BY UNDERGROUND EXPLOSIONS W. E. Townsend, Mark Langseth and B. Perkins, Jr. ERL Memorandum Report No. 1381 December 1961 DA Proj. No. 503-01-002, OMSC No. 5010-11-815 UNCLASSIFIED Report</p>
<p>Studies of crater dimensions versus shot depth have been made for sand and clay. By using a colored column technique, true crater dimensions and depths have been measured. Mineral and moisture content have been held nearly constant. Shear strength, grain size, soil density, cohesion and plasticity were measured. Accelerations of the ground particle versus distance were measured for shot depths varying from zero to 2 units of scale distance. The values of the acceleration at a given distance from successive explosions at the same depth had an average deviation from the mean value of approximately 25 per cent for both sand and clay. The average deviation of the crater dimensions was less than 10 per cent from the mean for sand and less than 5 per cent for clay.</p>	<p>Studies of crater dimensions versus shot depth have been made for sand and clay. By using a colored column technique, true crater dimensions and depths have been measured. Mineral and moisture content have been held nearly constant. Shear strength, grain size, soil density, cohesion and plasticity were measured. Accelerations of the ground particle versus distance were measured for shot depths varying from zero to 2 units of scale distance. The values of the acceleration at a given distance from successive explosions at the same depth had an average deviation from the mean value of approximately 25 per cent for both sand and clay. The average deviation of the crater dimensions was less than 10 per cent from the mean for sand and less than 5 per cent for clay.</p>	<p>Studies of crater dimensions versus shot depth have been made for sand and clay. By using a colored column technique, true crater dimensions and depths have been measured. Mineral and moisture content have been held nearly constant. Shear strength, grain size, soil density, cohesion and plasticity were measured. Accelerations of the ground particle versus distance were measured for shot depths varying from zero to 2 units of scale distance. The values of the acceleration at a given distance from successive explosions at the same depth had an average deviation from the mean value of approximately 25 per cent for both sand and clay. The average deviation of the crater dimensions was less than 10 per cent from the mean for sand and less than 5 per cent for clay.</p>
<p>AD Ballistic Research Laboratories, ARG MECHANICS OF CRATER FORMATION IN SAND AND CLAY PRODUCED BY UNDERGROUND EXPLOSIONS W. E. Townsend, Mark Langseth and B. Perkins, Jr. ERL Memorandum Report No. 1381 December 1961 DA Proj. No. 503-01-002, OMSC No. 5010-11-814 UNCLASSIFIED Report</p>	<p>UNCLASSIFIED</p>	<p>Accession No. Ballistic Research Laboratories, ARG MECHANICS OF CRATER FORMATION IN SAND AND CLAY PRODUCED BY UNDERGROUND EXPLOSIONS W. E. Townsend, Mark Langseth and B. Perkins, Jr. ERL Memorandum Report No. 1381 December 1961 DA Proj. No. 503-01-002, OMSC No. 5010-11-815 UNCLASSIFIED Report</p>
<p>Studies of crater dimensions versus shot depth have been made for sand and clay. By using a colored column technique, true crater dimensions and depths have been measured. Mineral and moisture content have been held nearly constant. Shear strength, grain size, soil density, cohesion and plasticity were measured. Accelerations of the ground particle versus distance were measured for shot depths varying from zero to 2 units of scale distance. The values of the acceleration at a given distance from successive explosions at the same depth had an average deviation from the mean value of approximately 25 per cent for both sand and clay. The average deviation of the crater dimensions was less than 10 per cent from the mean for sand and less than 5 per cent for clay.</p>	<p>Studies of crater dimensions versus shot depth have been made for sand and clay. By using a colored column technique, true crater dimensions and depths have been measured. Mineral and moisture content have been held nearly constant. Shear strength, grain size, soil density, cohesion and plasticity were measured. Accelerations of the ground particle versus distance were measured for shot depths varying from zero to 2 units of scale distance. The values of the acceleration at a given distance from successive explosions at the same depth had an average deviation from the mean value of approximately 25 per cent for both sand and clay. The average deviation of the crater dimensions was less than 10 per cent from the mean for sand and less than 5 per cent for clay.</p>	<p>Studies of crater dimensions versus shot depth have been made for sand and clay. By using a colored column technique, true crater dimensions and depths have been measured. Mineral and moisture content have been held nearly constant. Shear strength, grain size, soil density, cohesion and plasticity were measured. Accelerations of the ground particle versus distance were measured for shot depths varying from zero to 2 units of scale distance. The values of the acceleration at a given distance from successive explosions at the same depth had an average deviation from the mean value of approximately 25 per cent for both sand and clay. The average deviation of the crater dimensions was less than 10 per cent from the mean for sand and less than 5 per cent for clay.</p>